Lumen Contouring and Retrospective Gating of Coronary OCT

November 17, 2009

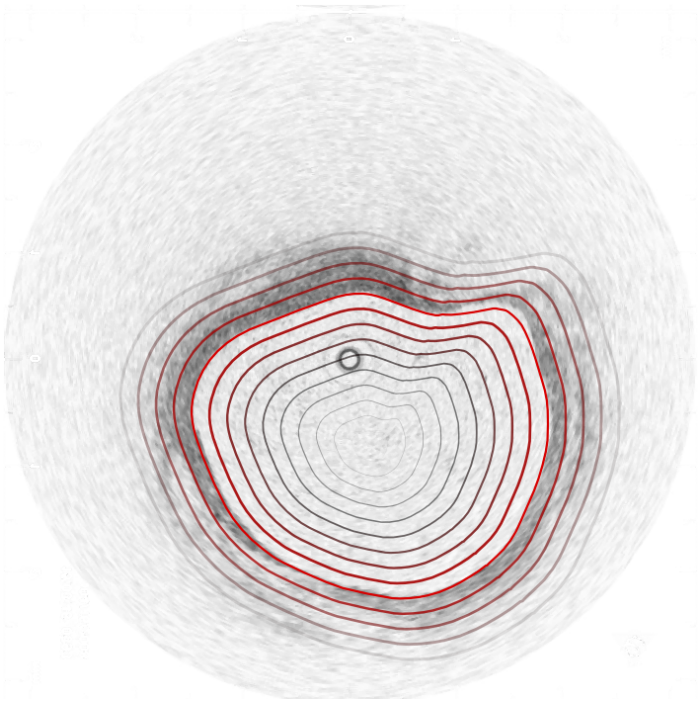

TU Delft
Delft University of Technology

Erasmus MC
University Medical Center Rotterdam

Preface

This report is a result of a master thesis project carried out at Erasmus Medical Center in Rotterdam. This master thesis is the final part of a Master of Science degree at Delft University of Technology.

The goal of this project was to develop and validate automatic lumen contour detection and an automatic gating algorithm. The resulting implementation should be usable for quantitative optical coherence tomography (OCT) analysis.

I would like to thank the following people: Nico Bruining for his endless support and insight. Charl Botha and Frits Post for their critical remarks and comments on all my writings. Sebastiaan de Winter for his ideas and remarks. Max Patijn for his support. My parents Frits Sihan and Boukje Gjaltema for their support and patience.

Abstract

Title of thesis:	Lumen Contouring and Retrospective Gating of Coronary OCT
Author:	Kenji Sihan
Date:	24 November 2009
Committee:	Prof. Dr. Ir. F.W. Jansen Prof. Drs. Dr. L.J.M. Rothkrantz Ir. F.H. Post Dr. C.P. Botha Dr. N. Bruining

Cardiovascular disease causes decreased blood flow to the heart and the brain. Due to the buildup of plaque the coronary arteries become narrow. The plaque can suddenly disrupt and partially or completely occlude a vessel, this can lead to myocardial infarction and sudden death. Angioplasty is a surgical procedure during which stents are placed inside the coronary arteries to keep these vessels open.

Quantitative analysis can be performed on an imaging technique called OCT to study the lumen areas over time and the effects of implanted stents. The lumen areas are the part of an artery where the blood flow through. Contour detection is necessary for calculating the lumen areas. To our knowledge the lumen contours of the coronary arteries from OCT data-sets are currently only manually detected, no method for automatic contour detection exists. The lumen volume can be calculated using the lumen areas and is also used in quantitative OCT analysis. However, motion artifacts are introduced due to the cardiac cycle while acquiring an OCT data-set. These motion artifacts reduce the accuracy of the calculated lumen volume.

The focus of this thesis is on automatic contour detection and selecting a subset of cross-sections is proposed as a possible solution for reducing these motion artifacts.

Contents

1 Introduction **3**

1.1 OCT imaging and Quantitative Analysis 3

1.2 Differences between OCT and IVUS 3

1.3 Overview of this work 4

1.4 Objective and Motivation 5

1.5 Terminology 6

1.6 Structure 7

2 Technology Paper **11**

3 Genetic Algorithm **41**

3.1 Crossover 41

3.2 Mutation 41

3.3 Alternative Encoding 42

4 The OCTour Software System **45**

4.1 Work-flow 45

4.2 Graphical User Interface 46

4.3 Locating Incorrectly Detected Contours 48

4.4 Repairing Incorrectly Detected Contours 50

5 Other Experiments **53**

5.1 Noise filtering 53

5.2 Single Collision Ray 54

5.3 Multiple Collisions Ray 54

5.3.1 Choosing Collision Points Using Shortest Path 56

5.3.2 Skipping points 56

5.4 Ray-casting discussion 57

6 Conclusion and Future Work **59**

6.1 Conclusions 59

6.1.1 Limitations 59

6.2 Future Work 60

Chapter 1

Introduction

The vessels that deliver blood to the heart are the coronary arteries. A buildup of fat inside the coronary arteries, also known as plaque, reduces the amount of blood that flows through the vessel. The plaque may disrupt and block completely or partially a vessel, this may lead to myocardial infarction. The plaque may also expand over time and slowly reduce the flow through a vessel. A patient with narrowed blood-vessels can receive pharmaceutical treatment or an intervention. This intervention consists of a balloon inflated inside the blood-vessel, the balloon is filled with water under pressure that pushes against the vessel wall such that the vessel wall expands. To prevent the weakened blood-vessel from collapsing a stent (a tube that prevents flow constriction) is implanted.

1.1 OCT imaging and Quantitative Analysis

Imaging techniques such as intravascular ultrasound (IVUS) and optical coherence tomography (OCT) are used to measure the volume of the lumen. OCT is an image acquisition technique based on infrared light that can be used to image the lumen of a coronary artery. To gather OCT data a catheter is inserted into a coronary artery and images are acquired while the catheter is pulled back at a constant speed. The images produced are cross-sectional images, also named cross-sections or frames, that are roughly perpendicular to the coronary artery wall. OCT is comparable to IVUS, which as the name implies is based on ultrasound for image acquisition.

If a blood vessel narrows then less blood can flow through at a constant blood pressure. New treatments for the coronary arteries are constantly being developed to prevent narrowing of the coronary arteries. As such it is important to measure the effect of the treatments on the lumen and to measure the area of the lumen.

1.2 Differences between OCT and IVUS

The axial resolution of OCT is higher than that of IVUS. An OCT (see fig. 1.1) cross-section contains more pixels in horizontal and vertical direction than an IVUS cross-section. The lumen contours are more pronounced due to the higher resolution and the lumen contours can be extracted more accurately from OCT data than from IVUS. An IVUS cross-section shows more of a vessel than an OCT

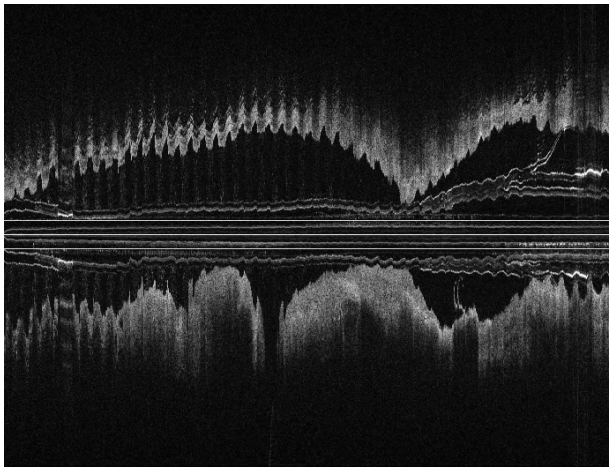

(a) An L-view of an OCT data-set. It clearly shows the lumen contour and saw-tooth artifacts.

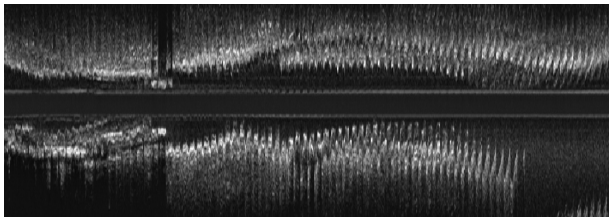

(b) An L-view of an IVUS data-set. It shows the lumen contour but it is not as detailed as the lumen contour of the OCT data-set.

Figure 1.1: Two L-views one of an OCT data-set and one of an IVUS data-set.

cross-section because ultrasound can penetrate vessel walls deeper than infrared light. The temporal resolution of IVUS is 30 cross-sections per second but the temporal resolution of OCT is only 15 to 20 cross-sections per second. However, newer OCT acquisition techniques can have much higher sampling frequencies [1].

1.3 Overview of this work

Two automatic lumen contour detection methods were developed. Improvements to both methods were applied based on the results of the detected lumen contours on 10 distinct cross-sections. These results were manually verified and used for quickly improving the contour detection implementations. The first method is based on ray-tracing (see section 5). Ray-tracing was difficult to improve such that it could deliver satisfactory results. The second contour detection method is inspired by ray-tracing. However, another approach is taken to avoid some of the problems we discovered with our implementation of ray-tracing. The second contour detection method was first tested on 10 OCT data-sets, consisting of a total of 1890 cross-sections, the results of this test are published in [2]. A second test with an additional 10 OCT data-sets was performed, consisting of a total of 4137 cross-sections, the results of this test are described in our accepted paper [3].

For quantitative analysis the lumen areas are used to calculate the lumen volumes. However, additional catheter movements due to the cardiac cycle and lumen expansion due to variable blood pressure [4] introduce noise to the calculation of the lumen volumes. Selecting a subset of cross-sections (gating) is proposed to suppress this noise. We formulated gating as an optimization problem to a binary high-dimensional problem and implemented a genetic algorithm (GA) to find an acceptable solution. The GA is compared to simulated annealing (SA). Matlab's implementation is used for SA. The lumen contours from OCT data-sets are often manually drawn, this is a tedious and time-consuming task. Cross-sections are selected at a fixed distance to reduce the amount of time required to complete this task, we named this selection method the fixed distance method (FDM). However, selecting cross-sections with the FDM is unlikely to reduce the amount of noise when calculating the lumen volume. A detailed description of the contour detection algorithm and the GA are described in our technology paper (see chapter 2).

An observer should be able to use the automatic lumen contour detection and gating algorithms for quantitative OCT analysis. OCTour is a software system (see chapter 4) developed for the observer to detect the lumen contours and gate the OCT data-set. The OCT data-set can be inspected in the longitudinal views and incorrectly detected lumen contours can be located. Several options are provided to correct these incorrectly detected lumen contours.

1.4 Objective and Motivation

Currently, coronary artery lumina are manually drawn in cross-sections of OCT data. This is a tedious and time-consuming task that requires the full attention of an observer. Furthermore, different observers can draw the same lumen contour differently. This is known as inter-observer variability. The same observer may also draw the same lumen contour differently, this is known as intra-observer variability. To our current knowledge, no automatic lumen contour detection method exists for OCT data of the coronary arteries. An automated lumen contour detection algorithm that correctly detects 90% of the contours in any OCT data-set is desired to solve these problems. The algorithm should be both empirically verified to work correctly and compared to the human performance for at least 20 OCT data-sets.

The lumen contour in an OCT cross-section is detected by our contour detection algorithm. The lumen volume is based on these detected contours. The physical area perpendicular to the blood-vessel wall corresponds to the axial direction of a cross-section. However, the line parallel to the blood-vessel may not correspond to the longitudinal direction of several cross-sections. This can be explained by empirical evidence of the saw-tooth artifacts which is observed in many OCT data-sets (see fig. 1.3). This saw-tooth artifact is caused by mixing the third (spatial) and fourth (temporal) dimensions into the third dimension of an OCT data-set. The catheter is slowly and automatically pulled back while imaging the blood-vessel at a constant velocity, the catheter may not move at a constant velocity relative to the artery. This effect is caused by the cardiac cycle. The heart moves, inflates/deflates and twists while the catheter slowly moves through the blood-vessel. The catheter moves relative to the pullback, this causes these saw-tooth artifacts clearly visible in a longitudinal view (L-view). Due to the cardiac cycle the catheter may move and rotate in both axial and longitudinal direction. Moving in longitudinal direction additional to the pullback may change the order of the

cross-sections. The lumen area changes during the cardiac cycle, the amount of change may depend on the blood pressure and the physical properties of the vessel wall. We would like to be able to accurately compare two lumen-volumes of OCT data-sets. For the reasons described above the saw-tooth artifact causes an inaccurate measurement of the lumen-volume [5].

During the end-diastolic phase of the cardiac cycle the heart is at rest. The catheter moves toward the same position during this phase and will potentially move very little relative to the pullback velocity. The end-diastolic cross-sections are the cross-sections that are imaged during the end-diastolic phase. We propose an algorithm that selects the (near) end-diastolic cross-sections from an OCT data-set. The lumen volume can be calculated based on only these end-diastolic cross-sections.

A large sample size is required to reduce the inaccuracy of calculating the lumen volume due to additional motion of the catheter relative to the vessel. The same problem exists for IVUS where it is solved by gating the data-set. IntelliGate [6] is used for gating IVUS data. Unfortunately it can not be directly applied to OCT data due to the difference in IVUS and OCT data (see section 1.2). IVUS captures more of a vessel because ultrasound can penetrate deeper into vessel walls than infrared-light. Certain features used in IVUS may not contain useful information to use for gating when applied to OCT because some features may rely on a large part of vessel walls being visible. The end-diastolic phase may also not be captured in OCT data. In this case the best that can be done is selecting cross-sections that are acquired close to the end-diastolic phase. The lumen contours may also be required for finding cross-sections (near) the end-diastolic phase because some features can only be extracted directly from the lumen contours (e.g. lumen area).

In this thesis we discuss our implementation for contour detection in OCT cross-sections. The contour detection algorithm requires a small initialization step. This greatly reduces the amount of work for observers who would otherwise need to draw the lumen contours manually. The result of our contour detection algorithm is compared to the result manually drawn contours. Furthermore, removing the saw-tooth shaped artifacts would facilitate the calculation of the lumen volumes from OCT data-sets. In this work, we address this problem with a method for automatic selection of cross-sections.

1.5 Terminology

The terminology used throughout this thesis is defined in this section.

The axial plane is the plane of cross-section of a vessel (fig. 1.2a). The longitudinal direction is perpendicular to the axial plane (fig. 1.2b).

Saw-tooth artifacts are most clearly visible in a longitudinal view (L-view) (see fig. 1.3). These saw-tooth artifacts are caused by the cardiac cycle. The cardiac cycle causes catheter movements and rotations to move relative to the pullback. The catheter movements consists of movements and rotation in the axial plane (fig. 1.4a). The catheter moves in the longitudinal direction (fig. 1.4b).

Gating is a selection of cross-sections from a data-set in such a way that the saw-tooth artifacts are removed or at least reduced. This is usually achieved by selection the near end-diastolic cross-sections. The end-diastolic cross-sections are the cross-sections closest to the end-diastolic phase. During the cardiac cycle the heart swells up before it is ready to pump the blood through the blood vessels.

Just before the heart pumps the blood through the blood vessels the heart is in rest, this is the end-diastolic phase.

The inside of a blood-vessel is called the lumen and the boundary around the lumen is called the lumen boundary. The lumen of a coronary artery is the part of the vessel where the blood flows.

1.6 Structure

In chapter 2 the technical details of both the contour detection and the gating are explained in our technology paper, to be submitted to a journal. The workflow of detecting the lumen contours is discussed using our application named OCTour in chapter 4. This chapter also provides an explanation of how to locate incorrectly detected contours if any are incorrectly detected and what how these contours can be corrected. Our earlier attempts at contour detection are explained in chapter 5. Our current contour detection is inspired by these earlier attempts. The limitations of the contour detection and gating are explained in chapter 6. This chapter also contains the conclusion and future work. The appendix includes two of our OCT-contouring publications. [2, 3]

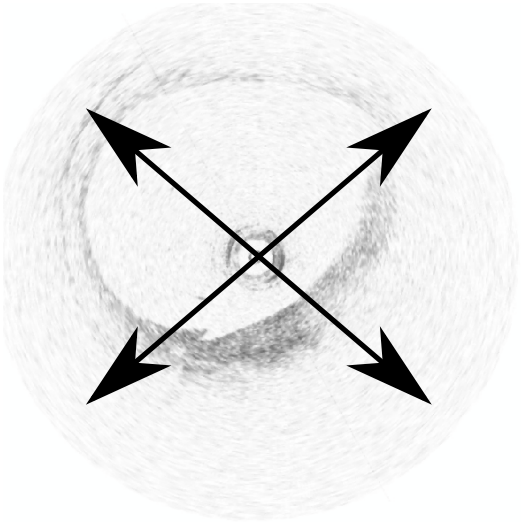

(a) Axial plane is on the cross-sectional area.

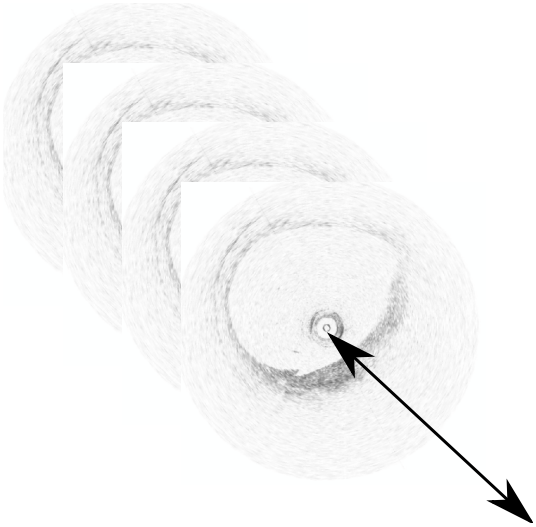

(b) Longitudinal direction is perpendicular on the cross-sections.

Figure 1.2: The axial plane and longitudinal directions.

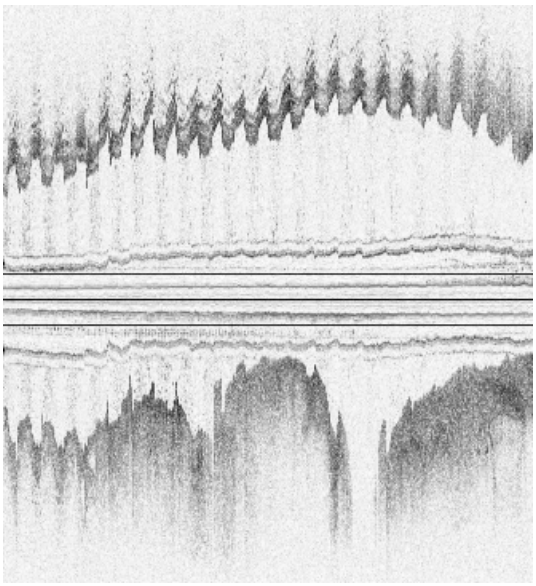

Figure 1.3: Saw-tooth artifacts are caused by the cardiac cycle and a slow pull-back speed.

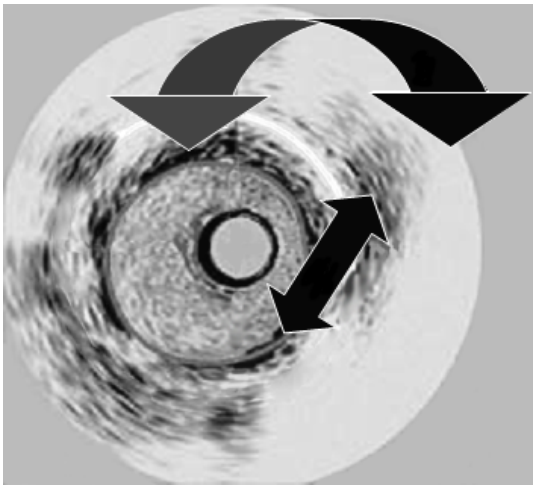

(a) The catheter moves and rotates in the axial plane.

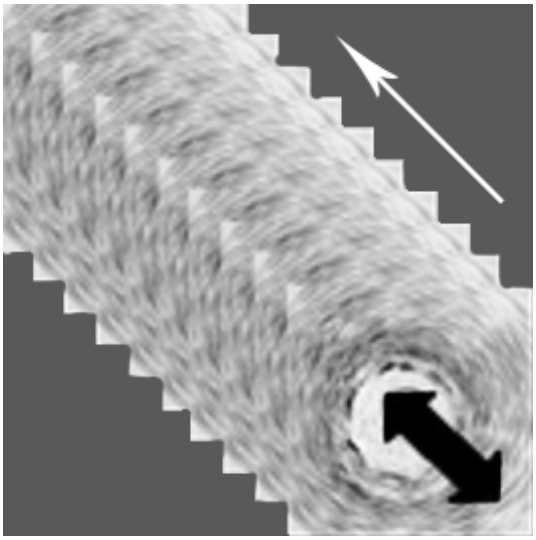

(b) The catheter moves in the longitudinal direction.

Figure 1.4: Catheter movements additional to the pullback movement.

Chapter 2

Technology Paper

This technology paper is a separate work, to be submitted to a journal. The techniques used for contour detection and gating are here described in detail and as such are part of this thesis. This technology paper describes the core ideas and algorithms of this thesis. The other chapters of this thesis contain supplementary material that expand on the topics discussed in the paper. This technology paper still refers to 10 OCT data-sets because at this time our paper [3] has been accepted but not yet been published, unlike this thesis that refers to 20 OCT data-sets.

Lumen Contouring and Retrospective Gating of Coronary OCT

Authors

November 13, 2009

Abstract

In this paper we propose a method for automatic optical coherence tomography (OCT) lumen contour detection and automatic (near) end-diastolic cross-section selection. Automatic lumen contour detection for OCT obviates the need for tedious manual contouring.

Manual contouring is usually applied to a subset of an OCT data-set because it can be too time-consuming to draw the contours for a complete data-set. Automatic contour detection can be applied to the entire OCT data-set. In this paper we document the technical aspects of our contour detection algorithm that was validated in our previous paper on 10 OCT data-sets containing a total of 1890 cross-sections.

The longitudinal-views of an OCT data-set show saw-tooth artifacts that may hamper accurate quantitative OCT analysis. In this paper we also propose an algorithm that removes the saw-tooth artifacts by selecting a subset of the cross-sections of an OCT data-set. This subset consists of cross-sections that are closest to the end-diastolic phase where the heart is at rest. The contours detected by our automatic lumen contour detection algorithm are used for selecting this subset.

1 Introduction

OCT is an imaging technique that has recently been introduced to visualize human coronary arteries [1, 2]. A small catheter with OCT transducer is inserted in a coronary artery and pulled back at a constant speed, thus producing images (see fig. 1 for an example). Images are generated as slices perpendicular to the coronary artery wall from inside the artery. The lumen contour is the interface between the area the blood flows and the coronary vessel wall. The amount of blood that can flow through a blood vessel wall is limited by this lumen area. The amount of oxygen directly correlates with the blood flow making the lumen area an important parameter. Narrowing of the lumen areas leads to a shortage of oxygen, which can result in myocardial infarction and death. An intervention can be performed on a patient with severe narrowing. This intervention usually consists of angioplasty, where a balloon inserted into the narrowed part of the coronary artery and inflated. Metal or the more recently bio-absorbable stents are implanted afterwards to prevent the weakened vessel wall from collapsing.

The change of the lumen areas is often used in studies to determine the effect of a new treatments. The acquired OCT data is a four dimensional object, three spatial mixed with one temporal dimension, this effect is also described by de Winter [3]. To acquire the OCT data-set a catheter is automatically pulled back at

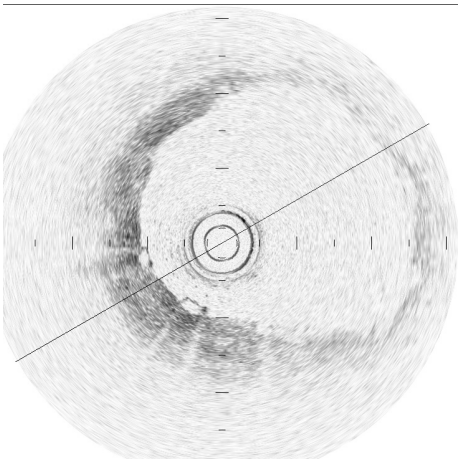

Figure 1: An inverted OCT cross-section, the overlay is shown in black.

a constant speed of 0.5 millimeter per second. Images are taken at a rate of 10 to 20 per second while the catheter is pulled through the coronary artery. A single OCT data-set can contain over 600 cross-sections. Longitudinal views (L-views) are generated by stacking all cross-sections from an OCT data-set and slicing through all cross-sections (fig. 3). L-views can give a comprehensive overview of a coronary artery. Unfortunately the heart is a dynamic organ that causes undesired motion effects. This causes saw-tooth shaped artifacts in OCT data that are clearly visible in an L-view. These saw-tooth artifacts are caused by catheter movements relative to the movement caused by the pullback and this can lead to measurement inaccuracies between multiple cross-sections. In previous work it was discovered that the catheter usually returns to the same position during the end-diastolic phase, during which the heart is completely filled and ready to pump the blood through the vessels [3]. Retrospective gating selects the cross-sections that are acquired during or near the end-diastolic phase whilst all other cross-sections are discarded, minimizing saw-tooth artifacts.

The lumen area and lumen volume are often used in quantitative OCT analysis. The lumen contour is used to calculate the lumen area. Currently, these lumen contours have to be manually detected. This is a tedious and time-consuming process that is also potentially sensitive to observer related bias. The solution we propose to this problem is to automatically detect every contour of an OCT data-set as described in section 3. The lumen areas are used to calculated the lumen volume. The accuracy of the lumen volume is hampered due to additional catheter movements. Selecting a subset of cross-sections (gating) can improve this accuracy. Our gating method for OCT data-sets is explained in section 4.4.

An automatic contour detection technique for OCT data is described in section 3. In section 4 an algorithm for gating based on the automatically detected lumen contours is proposed. In section 5 the results of our contour detection and gating algorithm are discussed. The conclusion is discussed in section 6.

2 Related work

A wide range of research on edge detection in general exists [4]. However, these general edge detection algorithms detect more edges than only on the lumen contour. A more specific edge detection for the lumen contour would be required. To the best of our knowledge there is currently no automatic lumen contour detection for OCT data-sets of the coronary arteries.

In this paper we share the technical details of our algorithm. In a previous paper [5], we described mainly the clinical aspects of this work. Hence, we give a detailed technical description of the techniques for lumen detection and selection of cross-sections in this paper.

3 Contour detection

Currently observers have to manually draw contours in every cross-section they want to use for quantitative OCT. Manually drawing contours is a tedious and time-consuming task that is virtually eliminated by our implementation of automatic contour detection. The detected contours can be used to calculate the lumen areas, this is an often used feature for quantitative OCT analysis. Another benefit of automatic contour detection is that it removes intra- and inter observer variability. Removing this variability improves the results of quantitative OCT analysis.

Automatic contour detection in an OCT data-set consists of three stages: noise filtering, contour detection and contour-refinement. In the noise filtering stage the speckle noise and overlay are removed from a cross-section before the contour detection step during which the actual lumen contour will be detected. After noise filtering, the lumen outlines are extracted in the contour detection step. The contour-refinement step will position the detected contour accurately on the lumen contour, gaps in contours will be filled using a circular arc interpolation and incorrectly detected contours will be flagged and replaced. An overview of the contour detection algorithm is shown in fig. 2.

3.1 Noise filtering

In the noise filtering stage a cross-section is prepared for contour detection. An overlay is sometimes added by the image acquisition device, this overlay hampers the contour detection. In step 1 (see fig. 5) the overlay is removed if present. A single specific mask would be insufficient to remove the overlay, because the overlay can be different depending on the OCT device which is used to acquire the OCT data and the settings of this device. Due to reflection of the infra-red light on the catheter, artifacts are clearly visible (see center of fig. 4a and 4c) in cross-sections. These artifacts are also in removed step 1. The results of every step of the noise filtering stage are shown in the figures from 4 to 7.

1. *Artifact removal:* Two circular masks (see fig. 4) are applied to remove catheter motion artifacts and mask pixels outside the imaged coronary artery. As the initial center, inner radius and outer radius are not automatically determined by our algorithm, the observer has to indicate these. The same center, inner and outer radius are applied to all cross-sections of an OCT data-set because the catheter center is fixed for all cross-sections and the

noise within inner radius and outside the outer radius varies only a little for all cross-sections. The inner radius and center are used to apply the inner circular mask. The center of the outer circular mask is the same as the inner circular mask. The inner circular mask removes catheter artifacts in the center of a cross-section. The outer circular mask removes any artifacts outside the lumen area.

2. *Speckle noise suppression:* A 7x7 median filter is applied (see fig. 5). This median filter removes the remaining parts of the overlay and also removes the speckle noise.

3. *Normalization:* The lower and upper parts of the intensity histogram are removed with a threshold in order to improve normalization of the cross-section. This step improves the normalization which brings the lumen contour into focus. A properly normalized cross-section will result in more consistent contour detection (see fig. 6).

4. *Contour smoothing:* A Gaussian filter is applied with $\sigma = 10$ pixels (see fig. 7). This is more than enough in practice to remove any irregularities and close small gaps in the lumen contour. A smaller σ may not close enough small gaps and may not remove enough irregularities. If the σ is set too small then too many edges may be detected which may hamper accurate edge selection (see section 3.2.4). A larger σ may smooth away some important details. In section 3.3 the contour is refined to recover details that were smoothed away.

The result of the noise filtering steps is shown in fig. 3.

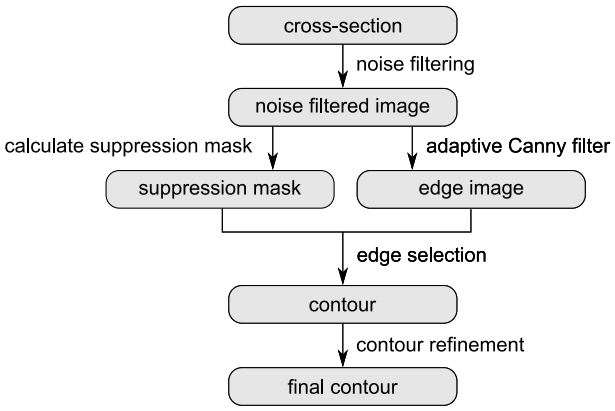

Figure 2: In this figure an overview of the automatic contour detection is shown. The nodes represent data and the arrows represent algorithms applied to the data. The node at the start of an arrow represents the input for an algorithm and the node at the end of an arrow represents the result of an algorithm.

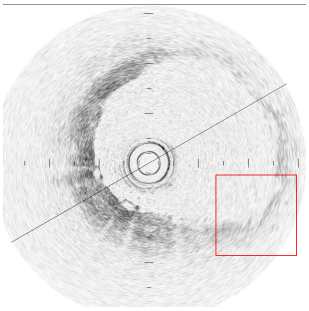

(a) Original cross-section, only the highlighted part of this image will be shown for the result of the noise filter steps.

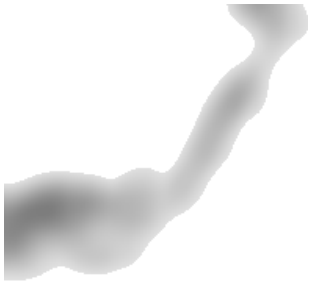

(b) Result after all noise filtering steps.

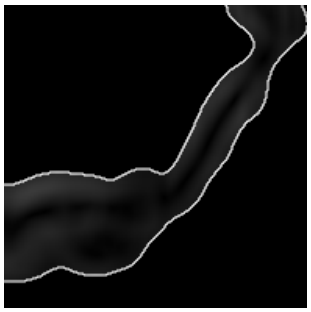

(c) Result of gradient magnitude applied to fig. B. This is just for illustration and is not used in the contour detection algorithm.

Figure 3: In fig. A the original cross-section is shown. In fig. B the exploded cross-section after all the noise filtering steps is shown (exploded section is highlighted in fig. A). In fig. C the gradient magnitude of fig. B is shown to illustrate the sharp and smooth edges produced as a result from fig. B.

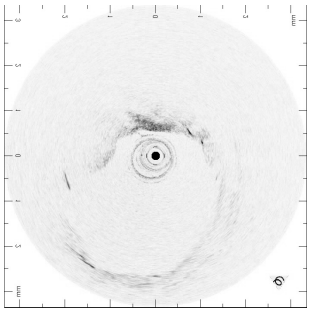

(a) Cross-section before application of the mask.

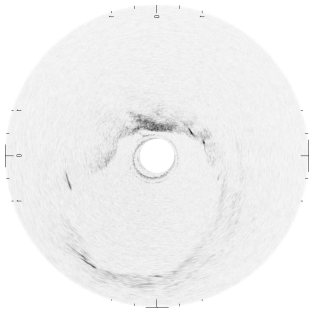

(b) Original cross-section after the mask is applied.

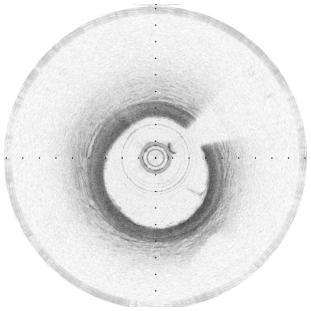

(c) This cross-section from another OCT data-set contains artifacts radially behind the outer radius of the suppression mask.

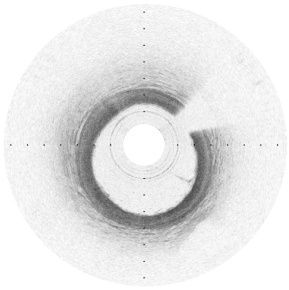

(d) The ring artifact radially outside the vessel is removed by the suppression mask.

Figure 4: Artifacts around the catheter and radially behind the lumen area are removed by application of two circular masks.



Figure 5: The overlay which is present in some OCT data-sets is removed using a 7x7 median filter. This median filter simultaneously removes some of the speckle noise.

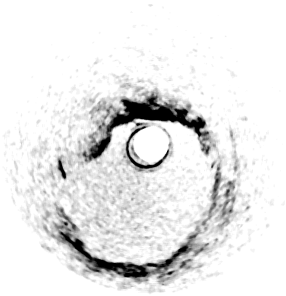

Figure 6: A normalized cross-section, the intensity is stretched over the entire histogram to make the contour detection more robust. All values are remapped to a range of $[0, 1]$.



Figure 7: To smooth the lumen contour a Gaussian filter with sigma 10 is applied to the cross-section. The filter is set this strong to filter out the small irregularities of the lumen contour.

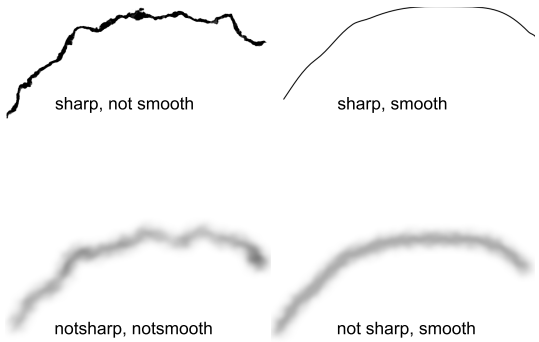

Figure 8: Sharp and smooth are orthogonal properties for contours. Sharp contours are contours that are more clearly visible. Smooth contours are less irregular, more continous.

3.2 Contour Detection

In this section our implementation of the contour detection will be discussed. The adaptive Canny filter (see section 3.2.1) detects all edges in the cross-section, including the edges that do no lie on the lumen contour. A suppression mask (see section 3.2.2) will then be calculated and applied (see section 3.2.3) to remove many edges that do no lie on the lumen contour and edges that are radially behind the lumen contour. A selection is made of the remaining edges 3.2.4 because not all of the remaining edges may lie on the lumen contour. In section 3.3 the contour refinement is discussed, this step improves the detected contour.

3.2.1 Adaptive Canny filter

The Canny filter [6] is used to detect all edges in the cross-sections, including edges that do not belong to the lumen contour. An edge is a sequence of connected pixels detected by the Canny filter. Two important parameters for the Canny filter are the upper and lower thresholds. The lower threshold is set to 40% of the upper threshold as recommended by Canny. The upper threshold for the Canny filter will be referred to as threshold. Another parameter in the Canny filter is the sigma. The sigma is set to 1 in this algorithm. This value is set to the same value for every data-set because the noise in the cross-sections has already been filtered. The threshold determines the sensitivity of the Canny filter, a lower threshold will detect more edges and a higher threshold will detect fewer edges. Due to variations between cross-sections an iterative scheme is used instead of a fixed threshold (see alg. 1 for pseudo-code). The threshold is calculated based on the percentage of pixels detected. If too few pixels are detected then the threshold is lowered to detect more, and if too many pixels are detected the threshold is raised. An iterative binary search is used to set the threshold for the Canny filter.

3.2.2 Suppression mask calculation

The suppression mask (see fig. 9) is used to remove edges that are radially behind bright areas that are detected by the Canny filter. Edges on the lumen boundary are radially in front of bright areas because the lumen is at the center of a blood vessel. Any edges behind the bright areas do not belong to the lumen boundary.

Algorithm 1 Pseudo-code for the adaptive Canny filter used to detect the lumen edges in a cross-section. Where lb and ub are the lower and upper-bound respectively, canny is the Canny filter with the parameters (upper threshold, lower threshold, sigma), imax is the maximum number of iterations, delta is used to calculate the difference for decreasing or increasing the threshold, T is the threshold and np is the number of pixels detected by the Canny filter divided by the number of pixels in the image. The division by the number of pixels in the image is to ensure that the boundaries work on different image resolutions. The constant 0.4 is the 40% for the lower threshold as recommended by Canny [6].

```
T := 0.5
target := (lb+ub)/2
i := 0
delta := 0.5
repeat
  np := canny(T, T*0.4, 1)
  if np<target then
    T := T-delta
  else
    T := T+delta
    delta := delta/2
    i := i+1
  end if
until (np<lb or np>ub) and i<imax
```

The following steps are used to create the suppression mask. The noise filtered cross-section from section 3.1 is used as input:

a *Gaussian filter:* Small irregularities in the cross-section on the lumen boundary may result in a large change in the orientation of the gradient vectors. The Gaussian filter is applied to smooth these small irregularities. This effect becomes apparent when the lumen intensity is low and the noise level is high relative to the lumen intensity.

b *Dot product:* The suppression mask is calculated based on the image gradient $[v_x, v_y]$ with the user-specified catheter center $[c_x, c_y]$. The dot product is calculated for every pixel as follows:

$$s = v_x c_x + v_y c_y \tag{1}$$

where s is the value of the suppression mask, $v = [v_x, v_y]$ is the gradient vector and $c = [c_x, c_y]$ are the coordinates for the center of the catheter (see fig. 9b).

c *Dilation:* A threshold is applied to image and the result is dilated (see fig. 9c).

3.2.3 Application of suppression mask to adaptive Canny filter

The edge selection step (see section 3.2.4) of the contour detection algorithm performs better when applied to fewer edges. The suppression mask removes as many edges as possible that do not lie on the lumen contour. Three steps are used to apply the suppression mask to the results of the adaptive Canny filter. Incorrectly detected edges, edges that do not lie on the lumen contour, are considered false



(a) The result of the noise filtering is used as input for the suppression mask.

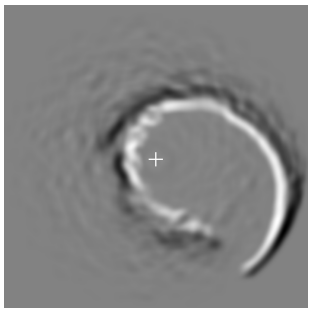

(b) The result after application of the dot product using the center of the catheter (indicated with a white cross) as center.



(c) The resulting suppression mask.

Figure 9: A visual overview of the steps used to create a suppression mask.

positives. Due to noise many of the detected edges can be false positive. These false positives are removed in step *a*. Due to small gaps in the lumen contour the detected edges on the lumen contour may be disconnected. In step *b* these edges will be merged. Reflection of infra-red light on the sheath of the catheter causes increased levels of noise around the center of the catheter. Special care is taken in step *c* to remove this noise. A more detailed explanation of every step is given in the following list:

a *Extraneous edge removal:* The suppression mask from section 3.2.2 is applied to the result of adaptive Canny filter from section 3.2.1 (see fig. 10). The adaptive Canny filter detects all edges, including the edges which are not on the lumen boundary, such as edges radially behind bright areas. The suppression mask removes all edges radially behind bright areas when applied to the image from the adaptive Canny filter. Any edges that are both smaller than 95% of all edges and are smaller than 20 pixels are edges we consider false positives, these edges are removed. Most of these edges are from speckle noise and are only three to ten pixels long. However, some cross-sections contain little speckle noise and as a result no edges are detected from speckle noise. If only edges smaller than 95% of all edges are removed and none of these edges originate from speckle noise then a longer edges can be removed as a result. These longer edges may lie on the lumen contour so these should not be removed. An upper bound of a length of 20 pixels ensures that longer edges will be preserved.

b *Edge fusion:* The result of the previous step is dilated, edges close to each other will be connected. The dilation used in this step uses a circular structuring element with a radius of N pixels, in practice $N = 7$ is large enough to connect



(a) Edges detected by adaptive Canny filter (see section 3.2.1).

(b) Suppression mask from section 3.2.2.

(c) Application of suppression mask with edge-image, some extraneous edges are still present in this image but these will be removed in the following steps.

Figure 10: Extraneous edges are removed from the edges detected by the adaptive Canny filter by combining it with the suppression mask described in section 3.2.2.

most edges on the lumen boundary. A relatively large disk ensures that small gaps in the contour will be closed. These edges are thinned and junctions of 3 or more edges are separated (see fig. 12). This step is shown in fig. 11.

c *Catheter edge noise suppression:* All edges that are over 90% to 110% of the catheter radius (user specified) are removed. The catheter at the center of a cross-section causes catheter artifacts. More and brighter speckle noise is caused by reflection on the catheter. Therefore, extra care is taken to remove edges which lie mostly within the user-specified radius around the center of the catheter.

3.2.4 Edge selection

This step uses the result of 3.2.3 (i.e. the edge image with suppression mask applied). Even though many edges are removed it is still possible that some of the detected edges do not lie on the lumen contour. In this step the edges that are likely to produce a correct lumen contour will be selected. The following steps are taken to select the edges for a contour:

a *Number of edges limitation:* The n longest edges are kept the rest is discarded. The longer edges are less likely to be detected due to noise in the cross-section. In our experience, $n = 12$ appears to be a good choice.

b *Edge selection:* For all combinations of edges select the edges that produce the contour with the highest quality score. Quality score is based on: area, length (relative to area), gaps in the contour (relative to length). A weighted average is taken to calculate quality score.

3.3 Contour-refinement

Noise filtering sometimes narrows the lumen contour. The exact amount varies from cross-section to cross-section but it is usually just a few pixels. The contour refinement step smooths the contour to create a result that is closer to manually



(a) Edges after step b, the short edges are removed. Noise present in a cross-section often causes extraneous short edges to be detected in the adaptive Canny filter.



(b) Edges are fused to close gaps in the contour, this will improve edge selection due to fewer choices in the edges to select.

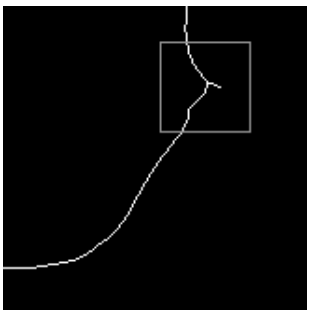

(c) The edges are thinned to create a 1px wide contour.

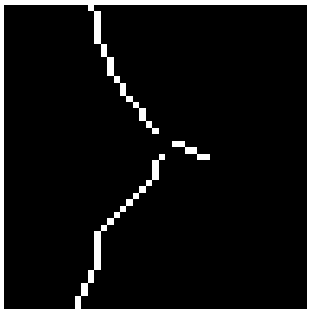

(d) One junction of three edges is separated into three edges.

Figure 11: Step 3: merge edges which are close to each other. Merging edges improves contour detection because it is more robust to select the correct edges when there are fewer edges to select.

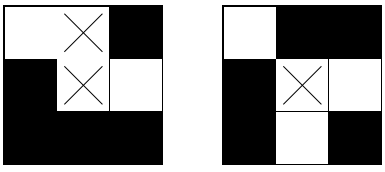

Figure 12: Two examples of breaking edges in 3x3 images. Detected pixels are white. Pixels which are surrounded by 3 or more detected pixels are marked for removal (here shown with a cross). T-junctions make it difficult to correctly form a contour.

drawn contours, which are smooth. The last correction in the contour refinement step replaces incorrectly detected contours with correctly detected contours.

3.3.1 Edge contour alignment

Detected contour points are moved radially outwards to the highest value on the suppression mask (see 3.2.2). Contour points are at most moved 10 pixels outwards. We observed that the lumen contour is within a distance of 10 pixels from the detected contour.

3.3.2 Contour smoothing

In this step the contours are smoothed in order to give visually similar results to the contours that are drawn by observers. The smoothing only takes place in the radial direction to preserve more details of the contour.

a Get suppression mask from 3.2.2 up to step 3.

b Contour points are only smoothed along the radius. The radius of all points of the contour are used as a linear signal that is smoothed. However, gaps in the detected contour are caused by branches and other artifacts in the coronary arteries. The contour is not smoothed over these gaps. Control points with a Euclidean distance greater than 3σ are ignored. If there are no gaps in the contour then this contour smoothing step behaves like a Gaussian smooth. A Gaussian smoothing is applied to the contour, where $\sigma = 5$ is large enough in practice to smooth the contour. The center used for smoothing of the contour is the centroid of the contour. The procedure can be mathematically described as:

$$\begin{aligned} \text{np} &= r_0 + \sum_{i=-3\sigma}^{3\sigma} \begin{cases} 0 & \text{if } |p_i - p_0| > 3\sigma \\ (r_i - r_0)G(i) & \text{otherwise} \end{cases} \\ G(x) &= \frac{1}{\sigma\sqrt{2\pi}} e^{-\frac{x^2}{2\sigma^2}} \end{aligned} \tag{2}$$

Where np is the smoothed point, σ is the amount of smoothing the contour, p_0 is the point to be smoothed, r_i is the radius of point p_i, G is the Gaussian filter and $|p_i - p_0|$ is the Euclidean distance between the points p_i and p_0. The index i is relative to the point to be smoothed on the contour (e.g. p_{-1} is the point before p_0 on the detected contour).

3.3.3 Circular interpolation

Due to branches in the coronary arteries the lumen contours contain large gaps. Observers smoothly interpolate these large gaps in contours. Gaps in contours need to be closed in order to accurately resemble manually detected contours. The following algorithm is used to interpolate gaps in contours (see fig. 13):

a *Center:* calculate the centroid of contour. The centroid is used because it's a simple and stable center relative to the detected contour.

b *Radius:* linearly interpolate radius from centroid of one end of the gap to the other end.

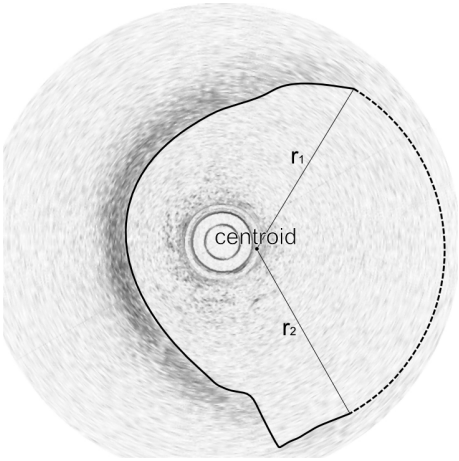

Figure 13: The dotted line is the line calculated using circular interpolation. The centroid is taken as center of the circle and r1 and r2 are used to calculate the radius at any point on the circle. Linear interpolation from r1 to r2 is used to ensure that the circle fits exactly in the gap.

3.3.4 Flag and replace

Incorrectly detected contours will be flagged and replaced by the closest correctly detected contour in the longitudinal direction. The lumen area is used to determine whether a contour is incorrectly detected. Incorrectly detected contours are flagged as follows:

a *Flag contours with threshold:* $D = \frac{\text{lumen area}}{\text{image area}}$, where lumen area is the area of the lumen of the detected contour and the lumen area is the area of the cross-section. If $D < \text{lowerbound}$ or $D > \text{upperbound}$ or $|\text{median} - D| > \text{threshold}$ then the cross-section is flagged, where $\text{lowerbound} = 0.02$, $\text{upperbound} = 0.80$, $\text{threshold} = 0.40$ and median is the median of five lumen areas from consecutive cross-sections around D.

b *Replace flagged contours:* flagged contours are replaced by the nearest non-flagged contour where closest is the shortest distance in longitudinal direction.

The parameters used in this contour detection algorithm were based on a small data-set consisting of 10 cross-sections. These cross-sections were selected to be distinct and cover potential problems for a contour detection algorithm (e.g. branches). The generalization of this algorithm was verified on 10 OCT data-sets containing a total of 1890 cross-sections of which also the manual contours were drawn by an observer [5].

The automatic lumen contour detection removes the tedious and time-consuming task for observers to manually draw lumen contours and enables contouring of complete OCT data-sets. The detected lumen contours can be used to calculate the lumen areas for quantitative OCT analysis. The next step is to calculate lumen volumes that can also be used in quantitative OCT analysis. However, reduced accuracy is caused by additional motion in the catheter due to the cardiac cycle. The solution we propose to improve the accuracy is to gate the data, select cross-sections that are imaged during the end-diastolic phase of the cardiac cycle. The heart is in rest during this end-diastolic phase which potentially eliminates additional catheter movements.

4 Gating

Saw-tooth artifacts due to catheter movements (see fig. 4.1) caused by the cardiac cycle (see fig. 15) can complicate quantitative analysis of OCT data-sets to be less accurate. To increase the accuracy of quantitative analysis on OCT data these saw-tooth artifacts have to be removed. Selecting a subset of cross-sections from the OCT data where the catheter potentially moves very little relative to the pull-back speed may reduce the saw-tooth artifacts. Some OCT data-sets do not show clearly visible sawtooth artifacts before gating (see fig. 14), these data-sets will not improve or improve very little after gating. The selected cross-sections are selected at points where the heart is in rest, the end-diastolic phase; we will call these the end-diastolic cross-sections. Due to a relatively short end-diastolic phase and a relatively low temporal sampling resolution some end-diastolic phases may not be imaged. In this situation the best we can do is selecting a cross-section that is nearest to the end-diastolic phase.

Features extracted from the detected lumen contours can be used to select the (near) end-diastolic cross-sections. We consider the following features useful for selecting end-diastolic cross-sections (see 4.3):

- The lumen areas are smallest during the end-diastolic phase due to lower pressure inside the lumen areas as described by Hiroshi Tsutsui *et al* [7].
- The catheter moves back to the original position relative to the pullback speed during every end-diastolic phase. The centroid of the lumen contour can be used to find catheter movements in axial direction.
- The coronary artery is expected to be more or less smooth in the longitudinal direction.
- All end-diastolic cross-sections are expected to be found at more or less regular intervals.
- The first and last end-diastolic cross-sections are expected to be within one cardiac cycle from the first and last cross-section.

For every selection a five terms are calculated (e.g. mean lumen area). These terms are based on the features that are extracted from the lumen contours. These terms are combined using a weighted mean in the fitness function, the result is one value that can be used to compare different selections. This suggests that the problem can be solved using optimization techniques.

OCT data-sets usually consists of more than 600 cross-sections. A selection of cross-sections is represented as a binary string with the length equal to the number of cross-sections. Every cross-section is potentially closest to the end-diastolic phase. Considering every selection makes finding the near end-diastolic cross-sections a binary high dimensional problem. Due to the high dimensionality of the problem domain we considered the following two methods to select near end-diastolic cross-sections: genetic algorithm [8] and simulated annealing [9]. We have implemented a GA and for comparison purposes we used Matlab's implementation of SA. In the following sections our implementation of the GA algorithm is documented.

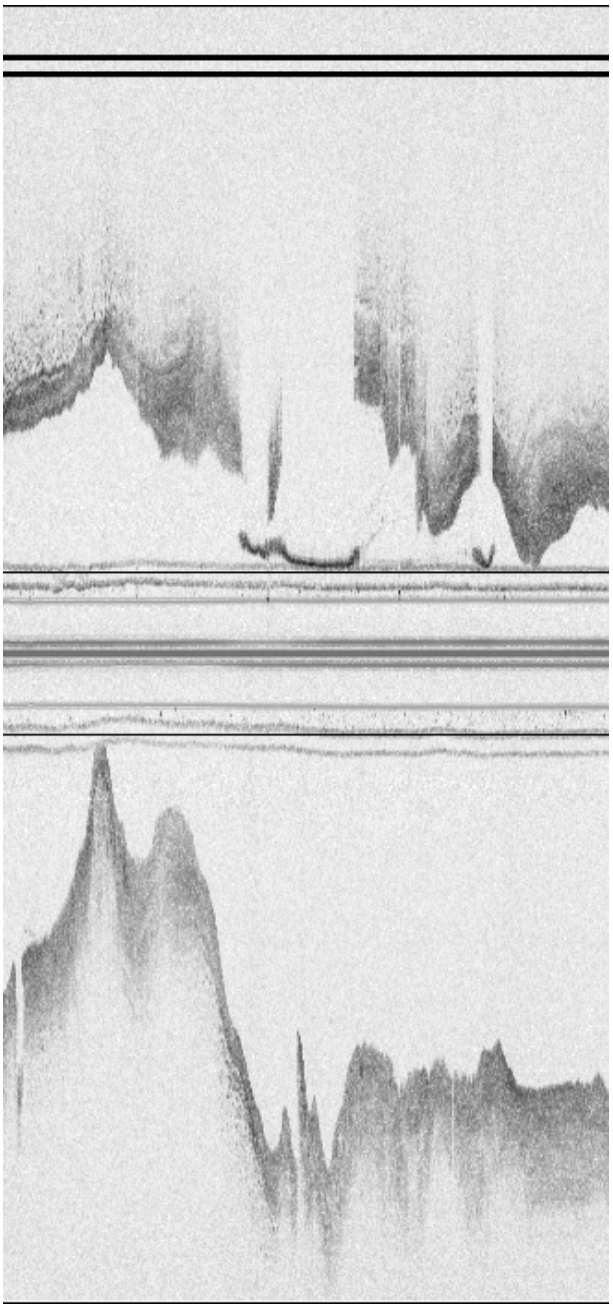

Figure 14: An ungated OCT data-set without the saw-tooth artifact.

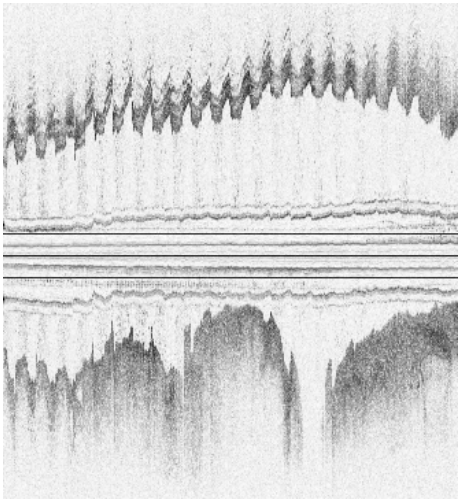

Figure 15: Saw-tooth artifacts caused by the catheter movements during the cardiac cycle additional to the pullback speed.

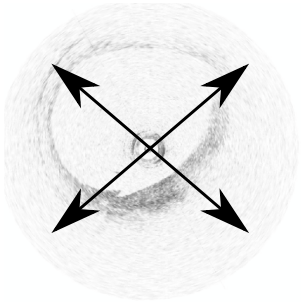

(a) Catheter movements in axial direction, these catheter movements are in the cross-sectional plane.

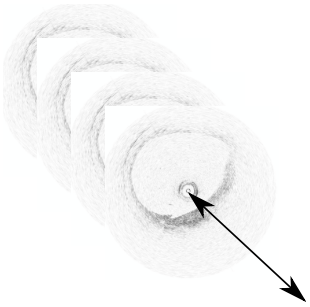

(b) Catheter movements in axial direction, these catheter movements are in the longitudinal direction.

Figure 16: Catheter movements relative to the pullback speed.

4.1 Catheter movements

The catheter moves (see fig. 16) and rotates in multiple directions during the cardiac cycle. These catheter movements cause the saw-tooth artifacts which can be seen in the longitudinal view of an OCT data-set (see fig. 15).

4.2 Estimating the cardiac rate

The cardiac rate can be used as a feature signal because two consecutive (near) end-diastolic cross-sections lie more or less at a distance corresponding with the cardiac rate. With a higher cardiac rate consecutive (near) end-diastolic cross-sections are closer to each other. However, the cardiac rate is rarely constant during a pullback but despite some variability the mean cardiac rate can still serve as a useful feature for determining the (near) end-diastolic cross-sections.

Due to a semi-regular cardiac cycle we expect that near end-diastolic cross-sections are at a more or less regular time interval from their neighbors. The mean cardiac

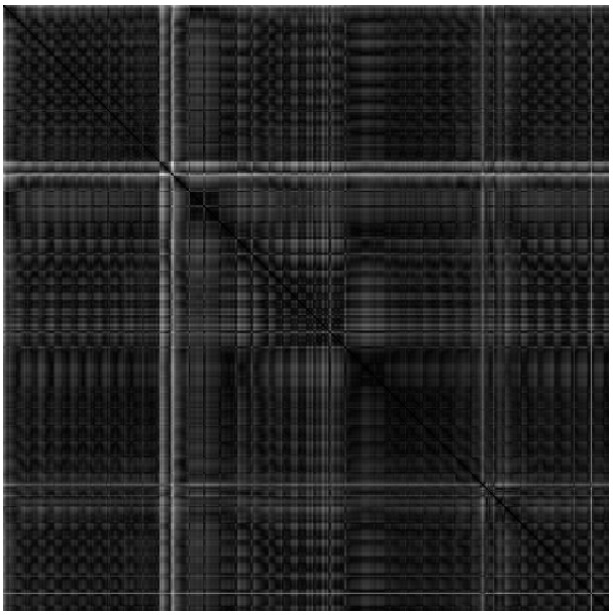

Figure 17: Dissimilarity matrix based on lumen area, center of gravity of lumen contour and roundness of the lumen contour.

rate can be used as a weighted term, the closer the selected cross-sections are to the mean cardiac rate the higher the weighted term.

A time interval is measured in a number of cross-sections between neighboring selected cross-sections plus one, the distance between cross-sections next to each other is 1. The mean cardiac rate for the longitudinal distance feature is measured in cross-sections per heartbeat. The higher the cardiac rate, the lower the expected mean longitudinal distance between selected cross-sections.

The cardiac rate is estimated based on multiple signals extracted from the automatically detected lumen contours. Every signal is filtered with a high pass Butterworth filter [10] and normalized to $[0, 1]$. Euclidean distance is used to calculate the dissimilarity matrix. From these signals a dissimilarity matrix is calculated that is used to estimate the mean cardiac rate as described by O'Malley *et al* [11]. Unfortunately, the dissimilarity matrix for most of the OCT data-sets we have contains much noise and artifacts (see fig. 17). However, it can still be used to determine the cardiac rate in cross-sections per cardiac cycle (see fig. 18). The signals which are used to estimate the cardiac rate are: contour area, centroid of the contour and roundness of the area (length divided by area).

4.3 Fitness function

The fitness function is used to compare two selections of the same data-set. A high value from the fitness function is an indication that the selected cross-sections are close to the end-diastolic phase. The fitness function is a weighted average based on the five weighted terms. A weighted mean is used to calculate the fitness function (see eq. 3).

$$\text{fitness} = \frac{1}{n} \sum_{i=1}^{n} wt \tag{3}$$

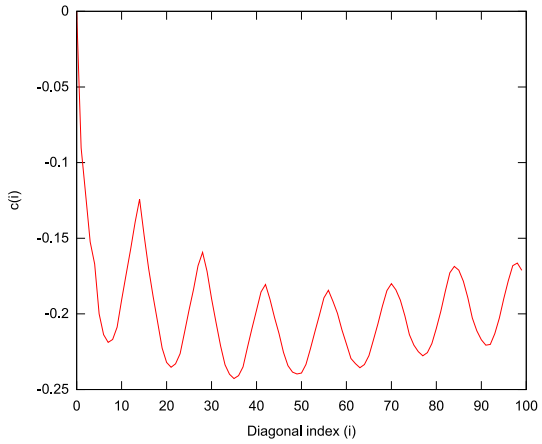

Figure 18: Dissimilarity index, the mean of a diagonal of the dissimilarity matrix. The diagonal (from top left to bottom right) is on index 0.

where $\mathrm{fitness}$ is the calculated fitness, n is the number of weighted terms (in our case $n = 4$), w is the weight for the weighted term and t is the value of the weighted term.

The weighted terms are calculated as follows:

- The mean of the lumen areas from the selected cross-sections is used as the weighted term. The lumen area is calculated using eq. 4, as described by Bourke [12]:

$$\text{area} = \frac{1}{2} \sum_{i=1}^{n-1} x_i y_{i+1} - x_{i+1} y_i \tag{4}$$

  where x and y are the x and y coordinates respectively of each point on the polygon, n is the total number of points and $x_1, y_1 = x_n, y_n$.

- The centroid coordinates are first normalized w.r.t. the image size so that $0 \leq x \leq 1$ and $0 \leq y \leq 1$ for all x and y coordinates. To remove any bias the mean of all x coordinates is subtracted from all x centroid coordinates, and similar for the y coordinates. The mean of the consecutive distances between selected cross-sections is used as the weighted term. As described in the introduction we expect that the catheter returns to the same position in every end-diastolic phase, when only considering the axial plane. Therefore, the centroid should return to the same position during every end-diastolic phase.

- The normalization is applied to the smoothness as is done for the centroid. But instead of the centroid four points on a smoothed contour are used. These points are the points above, below, left and right of the center of the catheter. The contour is smoothed as described earlier by eq. 2. The extra smoothing ensures a larger part of the contour is used than when only one point of the contour is weighted. We expect that these four points on a smooth contour return (nearly) to the same position during the end-diastolic phase.

- The distance between selected cross-sections is based on the cardiac rate, the number of cross-sections per heartbeat. The estimation of the cardiac rate is described in section 4.2. This signal is used because it is assumed that the cardiac rate is more or less constant during the pullback.

- The distance between the first selected cross-section and the first position and the distance between the last cross-section and the end position. Without this selecting only one cross-section could be optimal and we want to select cross-sections from the entire data-set.

4.4 Genetic algorithm

Our implementation of the genetic algorithm (GA) consists of 8 sub-populations where each sub-population consists of 25 individuals. The execution of the GA is divided over 50 iterations where each iteration consists of 500 sub-iterations. In total there are $50 \cdot 500 = 25000$ iterations for every sub-population. A new generation of each sub-population is created after a sub-iteration. After 500 sub-iterations the sub-populations swap out individuals with each other as described by Hu *et al* [13]. All sub-populations are sorted by their fittest individual. The ordering of populations is needed so the mutation and selection pressure rates per population can be calculated. The mutation rate for the least fit sub-population is set to 0.10 and is linearly interpolated to 0.04 for the fittest sub-population. The selection pressure is set to 0.5 for the least fit sub-population and is linearly interpolated to 3.0 for the fittest sub-population. These constants are based on experimental trial and error for one data-set and were tested on 11 more data-sets.

The quality function (see section 4.3) is used as a fitness function in the GA.

4.4.1 Initial population

The population of this GA consists of several sub-populations. Each sub-population is initialized with randomly generated individuals, except for one individual in every sub-population that consists of local minima of the lumen areas to speed up the GA. For all consecutive d cross-sections we select the cross-section with the lowest lumen area. Calculating this individual can be mathematically described as:

$$s_i = \begin{cases} 1 & a_i = \min(a_{i-c}, a_{i-c+1}, ..., a_{i+c}) \\ 0 & \text{otherwise} \end{cases} \tag{5}$$

where i is the ith cross-section of a data-set, a_i is the lumen area of the ithcross-section, $c = \left\lfloor \frac{d}{2} \right\rfloor$, d is the cardiac rate measured in cross-sections per cardiac cycle. A cross-section is selected if s_i equals 1 otherwise it is not selected.

4.4.2 Selection

The GA uses tournament selection to choose the fittest individuals. The selected individual is not removed from the population so it can be selected multiple times. Equation 6 is used to determine which individual to select where p is the selection pressure, n is the nth individual in the population and x is the probability that an individual is selected.

$$x = p(1-p)^n \tag{6}$$

As recommended by Hu *et al.* the selection pressure is dependent on the fitness of a population. The selection pressure of a population is lower when its fitness is lower. This allows the fittest population to focus on the best solution in the GA. The other populations will scout the search space to find a more optimal solution. This avoids the problem that one sub-population with a high selection pressure may lead to premature convergence of the GA and get stuck in a local optimum.

4.5 Simulated Annealing

The Matlab® implementation of simulated annealing (SA) is used with 200000 iterations and a temperature of $100/\,\text{iteration}$. To speed up the SA the first solution consists of an individual with locally optimal lumen areas (see section 4.4.1). The quality of a selection is determined by the quality function as described in section 4.3.

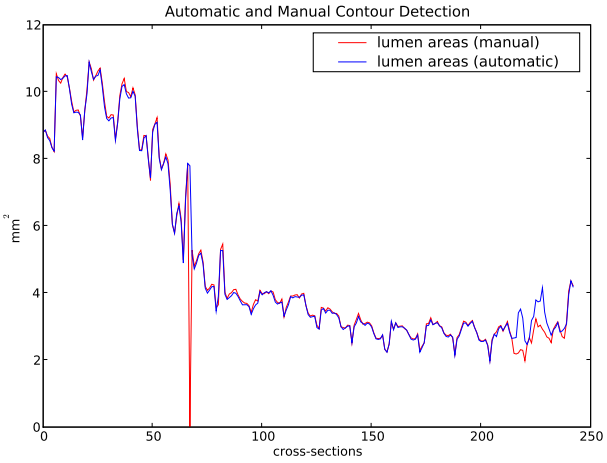

Figure 19: The lumen areas of manual contour detection compared to the lumen areas of the proposed automatic contour detection as described in this paper. Only a part of this data-set is manually drawn so only this part of this data-set can be compared against the automatic contour detection. For a more thorough validation based on 10 data-sets you can read our previous paper. [5]

5 Results and Discussion

5.1 Contour detection

The golden standard for contour detection consists of lumen contours manually drawn by observers. The automatically detected contours are compared to the manually drawn contours based on the lumen areas. Validation of the contour detection is performed on 10 data-sets as described in our previous paper [5]. The most important results are summarized here. Our implementation we utilize eight cores to speed the contour detection because the contour detection is a CPU intensive process. Currently it detects contours at a rate of 2 to 5 seconds per cross-section. The lumen area is an important feature of the lumen contour which is often used in studies, this feature is used for validation. From the 1890 compared cross-sections 10 (0.5%) lumen areas of the automatically detected lumen contours showed a large deviation from manually drawn lumen contours. Artifacts in the images on the sheath of the catheter caused these deviations. A graphical user interface is available to locate and correct these cross-sections. All other contour detected areas deviate $-1.14 \pm 1.87\%$ from the golden standard [5].

5.2 Cross-section selection

The cross-section selection (gating) is used to remove saw-tooth shaped artifacts visible in longitudinal views in OCT data-sets. These saw-tooth shaped artifacts hamper accurate quantitative OCT analysis because additional catheter movements are mixed into the OCT data-set. Cross-sections need to be selected such that these additional catheter movements are minimal. The catheter moves potentially very little relative to the pullback speed during the end-diastolic phase. The selected cross-sections that are the closest to the end-diastolic phase will minimize any additional catheter motion. The GA is compared to the SA and the fixed distance method (FDM). The fixed distance method is currently the most often used method to reduce the number of cross-sections from an OCT data-set. The

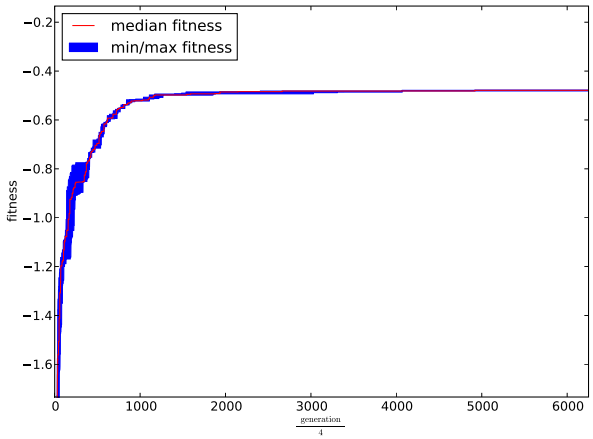

Figure 20: The fitness of the median individual, the minimum and the maximum during from five GA runs on the same data-set, where two of the most extreme values are discarded. As can be seen in this figure the fittest individuals from different GA runs converge. The GA is run for this many iterations to ensure that the fitness of the resulting selections will lie relatively close together.

GA and the SA are both methods used to optimize the selection of cross-sections such that the selected cross-sections are close to the end-diastolic phase. The FDM ignores any additional catheter movement, the time between any two consecutive selected cross-sections is constant. The performance of the GA and SA is discussed in sections 5.2.1 and 5.2.2, better performance implies a better selection of the cross-sections. If a selection method is more stable then less noise will be introduced during quantitative OCT analysis. The stability of the GA, SA and FDM is compared in section 5.2.3.

5.2.1 Performance of GA

The performance is measured using the quality function and the quality of the highest individual for a GA run. The primary concern of the performance is the quality at the end of a GA run. A higher quality results in a better selection of cross-sections. This is used to compare the GA with SA. Secondary is the convergence of multiple GA runs. If the GA converges poorly then the resulting selections will vary more than when the GA converges very well. Poor convergence will most likely result in poor stability, this is discussed in section 5.2.3.

5.2.2 Performance of SA

We executed the SA algorithm on the same data-set five times (fig. 21), it appears that SA does not converge even after reaching little or no improvement over a large number of iterations. SA does not seem to reach the same optimum as GA.

5.2.3 Stability of GA and SA compared to FDM

The GA and SA are stochastic algorithms, the solution can be different each time it is applied to an optimization problem. It is important to know how the variability of the GA and SA compares to the variability of the FDM. The FDM is an

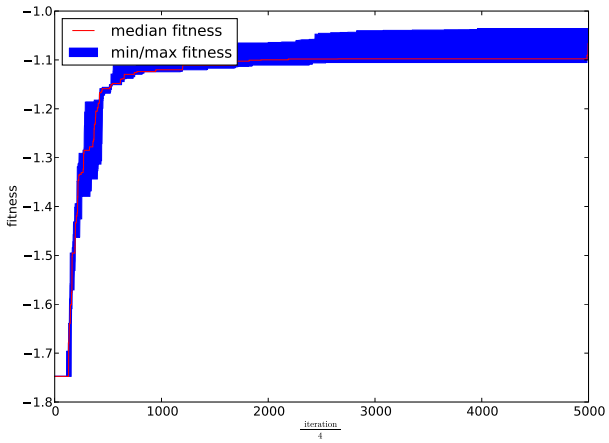

Figure 21: The fitness of the median individual, the minimum and the maximum during from five SA runs on the same data-set, where two of the most extreme values are discarded. As can be seen in this figure the fittest individuals from different SA runs do not converge. The SA is run for 200000 iterations.

often used method to calculate lumen volumes [7]. The result of five GA runs is compared against the result of the FDM where distance refers to the number of cross-sections between two selected cross-sections and not to the physical distance between two selected cross-sections. The FDM selects one cross-section every second (e.g. if the cross-sections are sampled with a rate of 15 cross-sections per second then every 15th cross-section is selected). Due to the cardiac rate and catheter movements relative to the catheter pullback speed the corresponding physical distance between the cross-sections selected with the manual method is unlikely to be constant. The GA attempts to select cross-sections where the distance between the selected cross-sections is constant. This is based on the assumption that the catheter moves very little relative to the pullback speed near the end-diastolic cardiac stage and that our current implementation is capable of selecting cross-sections near this end-diastolic stage.

Due to the stochastic nature of the GA and because the problem is a high dimensional binary problem the GA may not discover the global optimum. The number of dimensions is the same as the number of cross-sections in an OCT data-set, which can be over 600 for some data-sets. If two different OCT data-sets are taken from physically equal coronary arteries (e.g. two pullbacks from the same coronary artery with relatively little time between these pullbacks) then ideally the difference in measured mean lumen area should be equal as well. So an OCT data-set is compared to itself to measure the variability of the GA. In order to compare the variability of the GA to the variability of the FDM, different starting cross-sections are chosen for the FDM. With the FDM multiple distinct selections can be taken from the same data-set. The following two selections are examples with a sample rate of 15 cross-sections per second: [1, 16, 31, ...], [2, 17, 32, ...].

Both the GA and the FDM contain some noise in their measurements. The amount of noise per data-set is calculated as follows:

$$\text{noise} = \frac{\max(L) - \min(L)}{\min(L)} \tag{7}$$

where L is a list of the mean lumen area of every different selection. The larger the difference between the minimum and the maximum the less accurate a method is

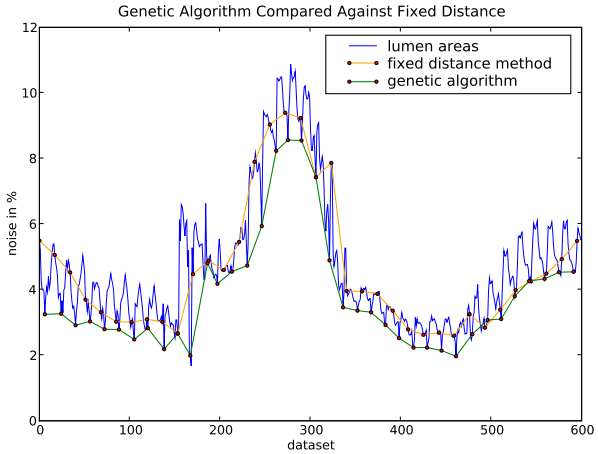

Figure 22: The lumen areas using a manual selection and the selection using the genetic algorithm.

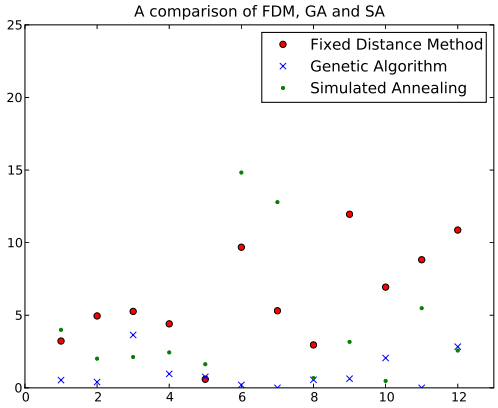

Figure 23: FDM compared to GA and SA for 12 different data-sets. The variability of different cross-section selection methods is measured using eq. 7. A lower variability implies a more robust gating method.

for the given data-set. Different gating methods and the FDM for all data-sets can be compared to each other based on this noise calculation (see fig. 23).

An example selection of both the manual method and the GA is shown in fig. 22.

5.3 Discussion of results

The performance of the GA and SA were discussed in the sections 5.2.1 and 5.2.2. The GA showed a higher and more consistent performance than SA. A higher performance results in a better selection of cross-sections and a more consistent performance of the GA implies more robust selection algorithm compared to the SA. These two optimizations algorithms are compared to the FDM that is currently often used to select cross-sections of an OCT data-set. The different cross-section selection methods are compared in section 5.2.3 on 12 data-sets. On 11 out of these 12 data-sets the variability of the GA is lower than the variability of the FDM (see fig. 23). There is only one data-set where the variability of the FDM is lower

than that of GA (see fig. 23data-set 5). In this data-set the variability of both methods is low compared to the other data-sets. In this case it may be difficult for a stochastic algorithm to achieve an even lower variability than that of FDM.

The GA and SA are both stochastic algorithms that introduce some variability given only limited time on a large binary optimization problem like gating. Perhaps the variability can be reduced with a local optimization algorithm instead of a global optimization algorithms like GA and SA. A local optimization algorithm may sacrifice a worse cross-section selection for reduced variability.

6 Conclusions and future work

In this paper we present the following two techniques:

- In this paper we share the technical details of our contour detection algorithm. The clinical aspects of this work are described in our previous paper [5]. Manual lumen contour detection for OCT data is a time-consuming task for the human observer. Automatic contour detection can reduce the time it takes to find the lumen contours. We have shown a robust automatic contour detection algorithm that is compared to the human observer for 10 different OCT data-sets imaged with different machines. The lumen contours are incorrectly detected on some cross-sections. However, these detected contours can be easily located and corrected by an observer. Automatic contour detection may be less susceptible to inter- and intra-observer variability than manual contour detection due to reduced human intervention.
- An automatic (near) end-diastolic cross-section selection technique is proposed to potentially improve the accuracy of calculation lumen volumes based on OCT data-sets. As demonstrated, selecting cross-sections with a fixed distance is likely to take cross-sections from any point of the cardiac cycle. Due to the catheter movements caused by the cardiac cycle the FDM introduces more variability than taking only cross-sections from the (near) end-diastolic phase. The proposed solution consists of approaching the cross-section selection problem as a global optimization problem that can be solved using a GA. The GA is compared to SA and to FDM. For SA the Matlab® implementation of the Optimization Toolbox™ is used. Our GA implementation turns out to be more stable and selects a better subset of cross-sections compared to SA and the FDM.

6.1 Limitations

For some cross-sections the lumen contour is incorrectly detected. However, these contours can be quickly located and fixed. Incorrectly detected contours are usually caused by branches in the coronary arteries. Detecting the lumen area with a branch correctly is difficult, especially when the lumen boundary is closed. Sometimes contours are incorrectly detected when the catheter touches the vessel wall. The artifacts around the center of the catheter coincide with the vessel wall and can be mistakenly detected as part of the lumen contour. Fortunately incorrectly detected contours are rare and easy to locate and correct.

Gating is used to improve the accuracy of calculating lumen volumes. Our gating algorithm has been verified on 12 data-sets out of 20 data-sets. Eight data-sets were discarded due to the absence of catheter movements that was apparent from the absence of saw-tooth shaped artifacts in the L-views. Plaque formation and calcification of the coronary arteries may lead to a reduced elasticity. As a result the lumen will not vary as much over the cardiac cycle this may contribute less pronounced saw-tooth artifacts.

6.2 Future work

Currently to our knowledge there is no golden standard for gating OCT data-sets. It would be possible to create a virtual environment and simulate an OCT

pullback. The physical properties of a coronary artery in this virtual environment would be known exactly and can be used to compare different gating methods accurately.

References

[1] Ulrich Gerckens, Lutz Buellesfeld, Edward McNamara, and Eberhard Grube. Optical Coherence Tomography (OCT). *Herz*, 28:496–500, 2003.

[2] M E Brezinski, G J Tearney, NJ Weissman, S A Boppart, B E Bouma, M R Hee, A E Weyman, E A Swanson, J F Southern, and J G Fujimoto. Assessing atherosclerotic plaque morphology: comparison of optical coherence tomography and high frequency intravascular ultrasound. *Heart*, 77:397–403, 1997.

[3] Sebastiaan de Winter. IntelliGate. Master's thesis, TU-Delft, 2003.

[4] Djemel Ziou and Salvatore Tabbone. Edge detection techniques - an overview. *International Journal of Pattern Recognition and Image Analysis*, 8:537–559, 1998.

[5] K. Sihan, C Botha, F Post, S de Winter, E Regar, R Hamers, and N Bruining. A novel approach to quantitative analysis of intravascular optical coherence tomography imaging. pages 1089–1092, 2008. http://www.cinc.org/Program/PC7-4.htm.

[6] J. Canny. A computational approach to edge detection. *IEEE Trans.*, 8:679–714, 1986.

[7] Tsutsui H, Schoenhagen P, Crowe TD, Klingensmith JD, Vince DG, Nissen SE, and Tuzcu EM. Influence of coronary pulsation on volumetric intravascular ultrasound measurements performed without ecg-gating. validation in vessel segments with minimal disease. *International Journal of Cardiovasc Imaging*, 19:51–57, 2003.

[8] John H. Holland. *Adaptation in natural and artificial systems*. MIT Press, Cambridge, MA, USA, 1992.

[9] S. Kirkpatrick, C. D. Gelatt, and M. P. Vecchi Jr. Optimization by Simulated Annealing. *Science*, 220:671–681, 1983.

[10] Stephen Butterworth. On the theory of filter amplifiers. *Wireless Engineer*, 7:536–541, 1930.

[11] Sean M. O'Malley, Juan F. Granada, and Ioannis A. Kakadiaris. Image-Based Gating of Intravascular Ultrasound Pullback Sequences. *IEEE TRANSACTIONS ON INFORMATION TECHNOLOGY IN BIOMEDICINE*, 12:299–306, 2008.

[12] Paul Bourke. Calculating the Area and Centroid of a Polygon. `http://local.wasp.uwa.edu.au/\~pbourke/geometry/polyarea/`, July 1988.

[13] Jianjun Hu, Erik D. Goodman, Kisung Seo, and Min Pei. Adaptive Hierarchical Fair Competition (AHFC) Model For Parallel Evolutionary Algorithms. In *GECCO '02: Proceedings of the Genetic and Evolutionary Computation Conference*, pages 772–779, San Francisco, CA, USA, 2002. Morgan Kaufmann Publishers Inc.

Chapter 3

Genetic Algorithm

This chapter provides more detail that is not described in our paper as well as a more general description of the genetic algorithm (GA). A GA is a search technique to find solutions for optimization of search problems. GAs are a class of evolutionary algorithms that are inspired by evolutionary biology. A GA population consists of multiple candidate solutions (individuals). Every individual represents a single solution to an optimization problem. These individuals are encoded as binary strings in our algorithm. The evolution usually starts with a population of randomly generated individuals. A fitness function is used to measure the quality of an individual. For each generation individuals are selected for the next generation. These individuals are combined using a cross-over operation.

A (sub)selection of cross-sections is represented as a bit-string (individual). Every '1' represents a cross-section that is selected while every '0' represents a cross-section that is not selected. The cross-over operation is a genetic mutation which for this problem combines two bit-strings while preserving subsets of these bit-strings. These subsets of the bit-strings may represent a higher fitness value when combined and result in improved individuals.

A population in a GA may get stuck in a local optimum with a low probability to escape. Therefore, several sub-populations are used with different mutation rates and selection pressures.

3.1 Crossover

The GA uses a two-point crossover function (see fig. 3.1) to combine two parents into one child. It is possible that the same parent is chosen twice in which case one parent will be identical to its child.

3.2 Mutation

Mutation in a GA is used to prevent a population from getting stuck in a local optimum. The number of selected cross-sections can be changed or cross-sections can be moved through the OCT data-set. Every cross-section has a probability p of being added/removed from the OCT data-set. This genetic operation is applied by flipping a bit in the bit-string (see fig. 3.2a). Cross-sections can also be moved

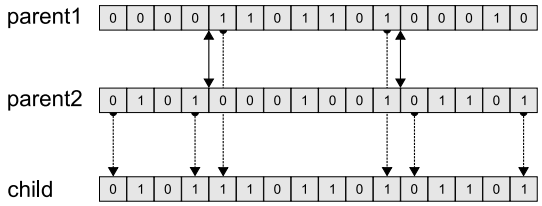

Figure 3.1: An example of two point crossover applied to two bit-strings and the resulting child are shown in this figure.

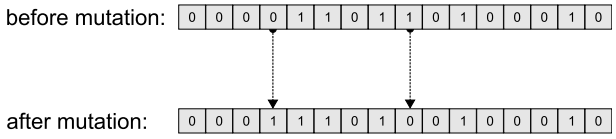

(a) This mutation adds one cross-section and removes one cross-section by flipping a bit.

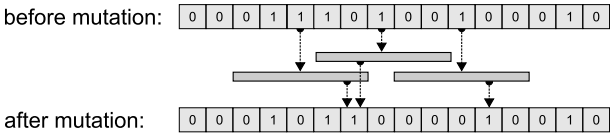

(b) Cross-sections are moved with this mutation in a data-set. The movement is limited to a fixed range using a uniform distribution. It is possible that multiple cross-sections are moved to the same position as shown in this figure, this will result in fewer cross-sections after the mutation.

Figure 3.2: An example of a genetic mutation operation applied to a bit-string and its results. (3.2a) The first mutation step shows adding/removing cross-sections from the OCT data-set. This requires flipping a bit. (3.2b) The second mutation step consists of moving a cross-section within a fixed distance. A cross-section is moved using a uniform distribution within a maximal distance of its current position.

through the data-set. This is done in two stages. In the first stage some cross-sections are selected with probability p; these cross-sections are marked for the second stage. The bits of the selected cross-sections are set to 0, these cross-sections are removed from the OCT data-set in this intermediate step. The new position of the marked cross-sections is determined by a uniform distribution within a fixed distance of the current position of each cross-section (see fig. 3.2b). In the second stage all new positions of cross-sections are set to 1. This two stage approach ensures that the order of moving the cross-section makes no difference for the result. If two cross-sections are moved to the same position then the two cross-sections become one.

3.3 Alternative Encoding

An alternative representation for individuals is encoding only each selected cross-section. The positions of each selected cross-section are encoded in a list of integers. The advantage of this approach compared to the bit-string encoding is that only the selected cross-sections need to be stored. The disadvantages of this

approach are:

- The cross-sections are not guaranteed to be sorted. This means that additional steps need to be taken to ensure the cross-sections are in the correct order.
- One cross-section can exist multiple times. Unlike the bit-string representation, duplicates may exist in a selection with this representation.
- The length of a selection is variable. For different selections of the same data-set it is possible that a different number of cross-sections is selected. The bit-string representation is always the same length for the same OCT data-set.

Due to these issues we selected the bit-string representation for representing individuals.

Chapter 4

The OCTour Software System

OCTour is an implementation of the described algorithms for automatic lumen contour detection and gating of OCT data-sets. This application contains a graphical use interface (GUI) to assist an observer in inspecting a data-set (see fig. 4.5).

4.1 Work-flow

This work-flow section provides an overview of how the lumen contours are detected from an OCT data-set.

1. An OCT data-set needs to be imported into OCTour (see fig. 4.1).
2. After an OCT data-set is imported the inner and outer masks need to be initialized. The inner mask is set by dragging from the center and dragging outwards until the radius of the inner mask is large enough. The outer mask is defined by positioning the cursor on the desired radius and clicking (see fig. 4.2).
3. The lumen contours are ready to be detected. By clicking on the button "Detect contours", the contour detection algorithm is started.
4. If necessary, incorrectly contours can be located and corrected. The L-views can be rotated (see fig. 4.3) to inspect the OCT data-set for incorrectly detected contours. A graph of the lumen areas and a quality metric are also shown (see fig. 4.5). The observer can jump to any cross-section in the data-set by clicking in an L-view or on the graph. To move forwards or backwards through an OCT data-set cross-section by cross-section the "." and "," keys are used.
5. If an incorrectly detected contour is located it can be repaired. Often just removing a part of the contour is enough but sometimes it is necessary to copy from the previous contour or the next, whichever would be a better fit. When these options are insufficient a part or even the entire contour can still be manually drawn. Any mistakes can be easily corrected by clicking the "undo" button or to start over with the detected contour by pressing the "reset" button.
6. If the data-set contains saw-tooth artifacts it can be gated using the "select cross-sections" button (see fig. 4.5). After a data-set is gated a vector with the selected cross-sections can be exported.

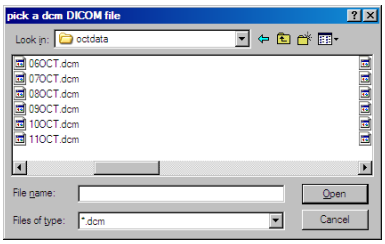

Figure 4.1: Select a DICOM file to import into OCTour.

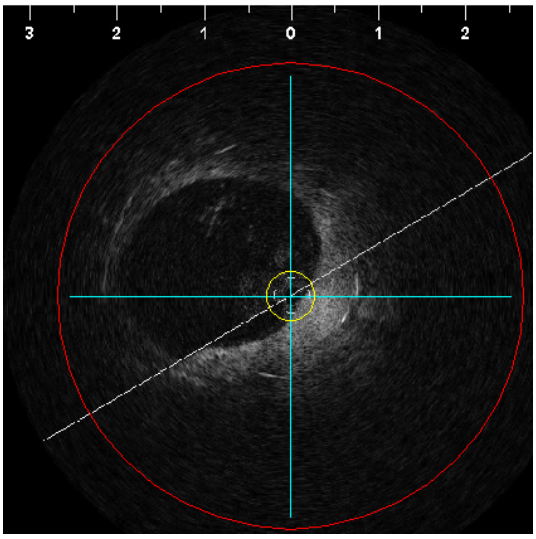

Figure 4.2: A cross-section with the inner (yellow) and outer (red) masks manually defined.

7. The contours are ready to be exported for quantitative OCT analysis. However, it is not always possible to extract the physical dimensions from a DICOM file that is required to calculate the lumen areas in mm^2. Manual input is then required to get these correct physical dimensions. The distance in mm has to be selected using the menu (see fig. 4.4). Two clicks in the cross-section corresponding to the selected distance are then required to determine the physical distance.

4.2 Graphical User Interface

The graphical user interface (GUI) can be used by observers to automatically detect the lumen contour, find and correct incorrectly detected contours and select the near end-diastolic cross-sections (see fig. 4.5). The result can be exported for quantitative analysis to CURAD [7]. The GUI is setup as follows:

On the left in the GUI is a single cross-section for correction and next to this cross-section are two L-views for navigating through an OCT data-set. Some cross-sections of an OCT data-set may be incorrectly detected by our contour detection algorithm. These incorrectly detected contours have to be manually corrected. The GUI offers support to locate and repair these incorrectly detected contours. After the lumen contours are detected and the data-set is gated it can be exported

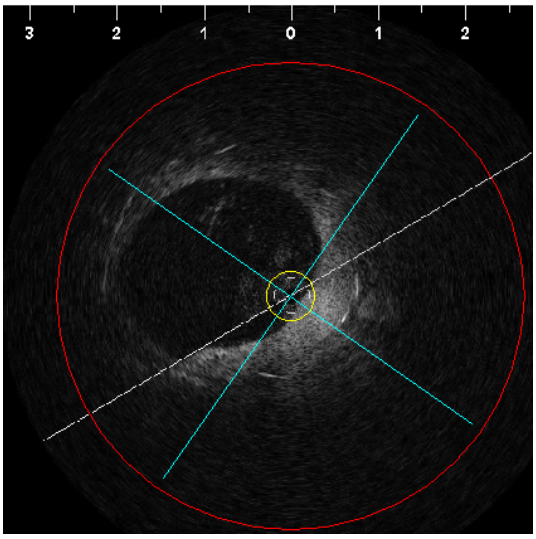

Figure 4.3: Rotating the L-views, the cyan lines through the center in cross-sectional view indicate the corresponding L-views.

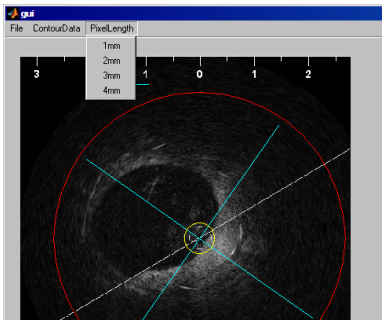

Figure 4.4: Select the distance in mm.

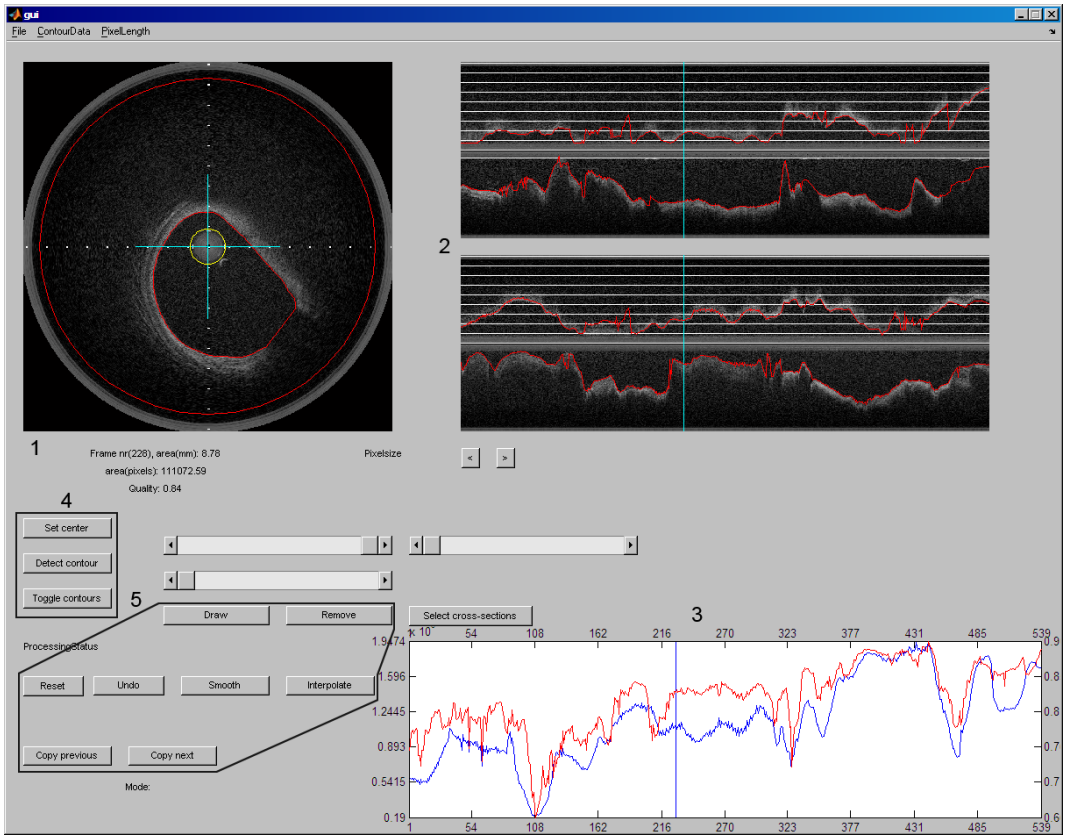

Figure 4.5: See section 4.2 for a description.

for quantitative OCT analysis in another application that is currently used for this task.

1. The currently selected cross-section.
2. L-views with indication of current cross-section and the detected lumen contours are shown after the automatic contour detection algorithm is applied to an OCT data-set.
3. Graphs of a contour quality metric (red) and the lumen area (blue). These can be used to find abnormal deviations possibly caused by incorrectly detected contours.
4. Buttons for initializing the contour detection, starting the contour detection and hide/show the detected lumen contours in the cross-sectional view and the L-views.
5. Tools for correcting contours when the contours are incorrectly detected.

4.3 Locating Incorrectly Detected Contours

The GUI shows the lumen area and a quality score based on the detected contour. An observer can locate incorrectly detected contours. In fig. 4.6 through fig. 4.8 an example is given for locating and correcting an incorrectly detected contour.

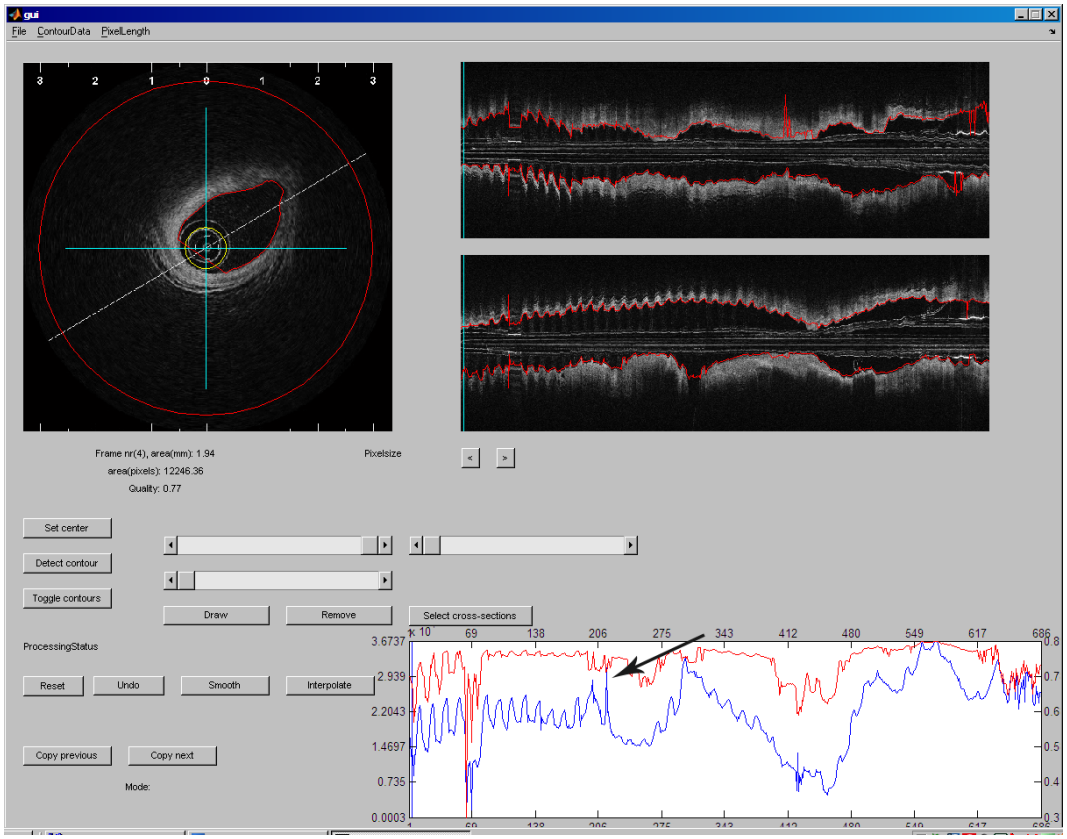

Figure 4.6: The black arrow indicates a spike in the lumen areas (blue line). Because the spike is pointing upwards a sudden large increase is present in the lumen areas. As we don't expect any large changes between consecutive in lumen areas between cross-sections clicking on this spike will show the cross-section with corresponding lumen contour.

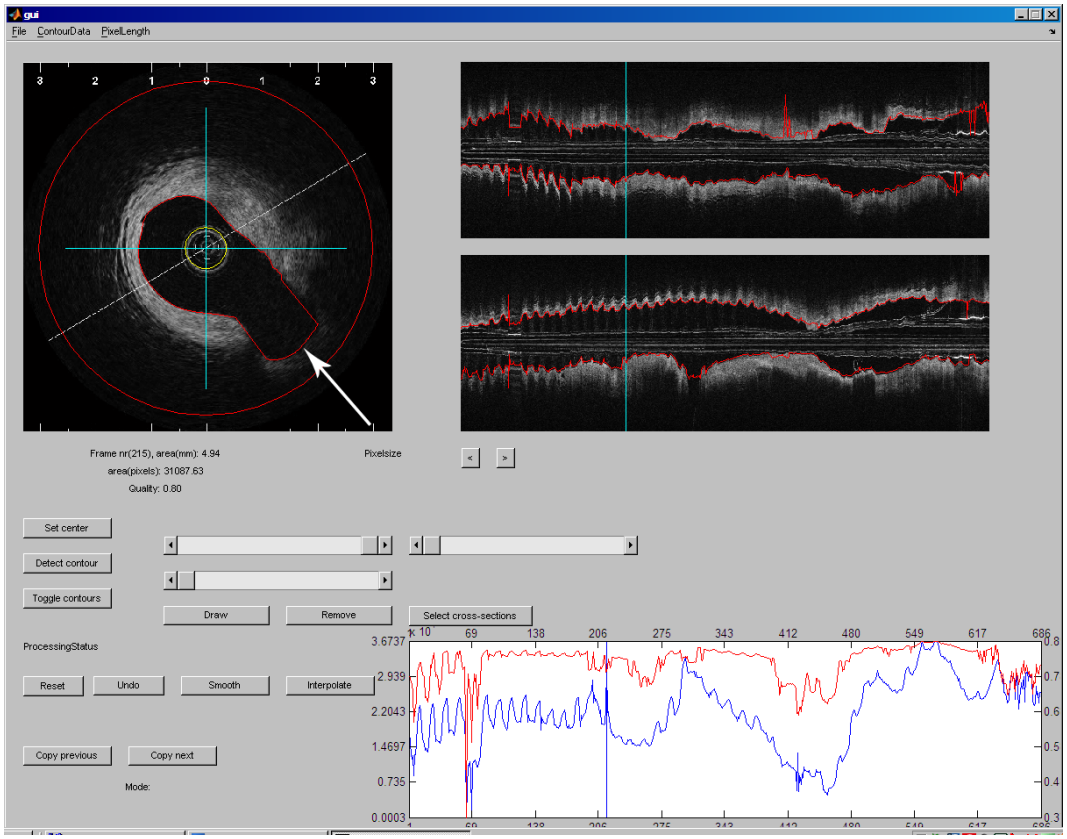

Figure 4.7: A part of the contour is incorrectly detected (here noted with a white arrow) detected due to a branch in the coronary artery.

4.4 Repairing Incorrectly Detected Contours

Multiple options exist to fix the lumen contours. A part of the lumen contour can be removed and closed by our circular interpolation algorithm (see chapter 2). The lumen contour may also be drawn manually, where some parts of the existing contour are replaced by the newly drawn contour.

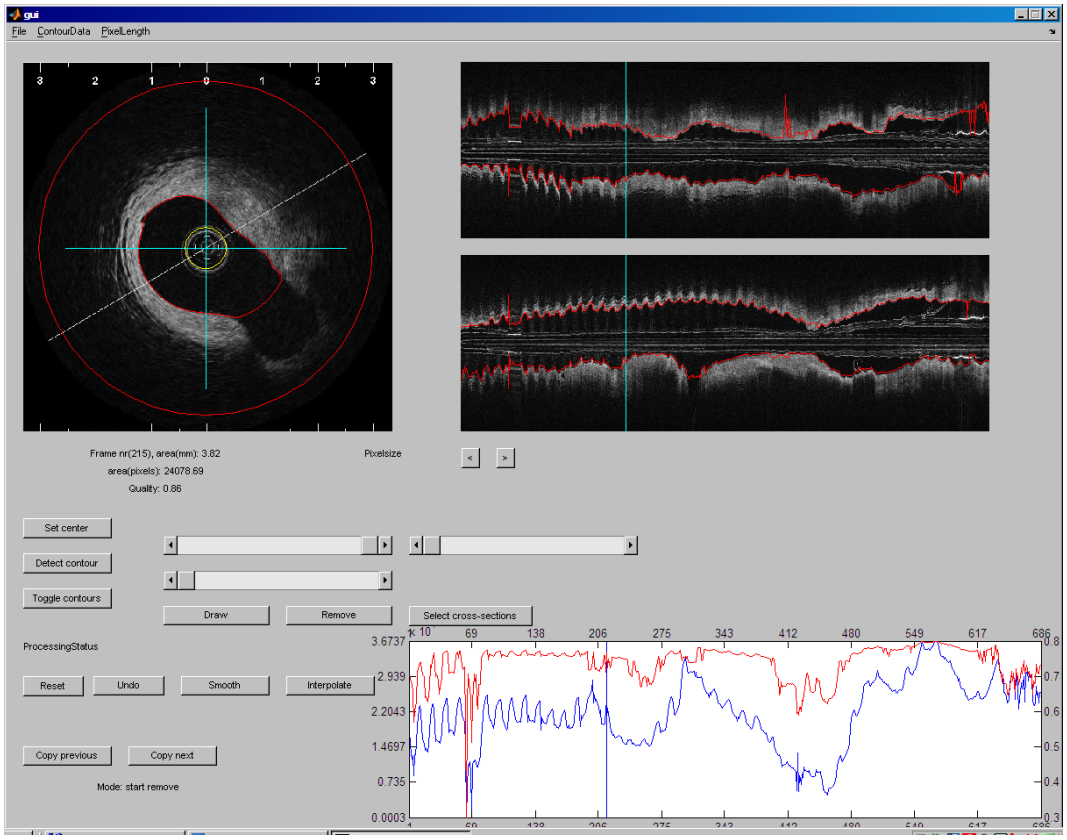

Figure 4.8: The “remove tool” is used to remove a part of the contour, followed by circular interpolation to close the gap.

Chapter 5

Other Experiments

This chapter provides background information of our current contour detection algorithm. This background information consists of a description of our previous implementation (based on ray-casting) for detecting the lumen contours. Ray-casting served as a source of inspiration for our current implementation (see section 2). The problems we discovered with ray-casting are described in this chapter, these problems are avoided with a new approach in our current implementation.

Our ray-casting algorithm was difficult to improve for multiple cross-sections. In particular removing contour points (see section 5.3.2) from rays that incorrectly detected the contour while keeping control points that lie on the lumen contour. Our implementation of ray-casting is sensitive to small artifacts and noise in a cross-section (see fig. 5.2) because rays independently detect contour points. The current contour detection algorithm is less sensitive to noise and to incorrectly detected contour points because all connected contour points (edge) are either included or excluded from the contour instead of single contour points.

In our ray-casting algorithm a ray starts from the center of the catheter and is cast towards the edge of the cross-section. Ray-casting in this implementation is limited to 5 degrees, 72 rays per cross-sections.

5.1 Noise filtering

Noise and other artifacts in OCT cross-sections needs to be filtered for robust contour detection. The following noise filtering steps are used based on trial and error in a small training data-set consisting of 10 OCT cross-sections:

- The overlay is removed using a 3x3 median filter.
- The lower end of the histogram containing most of the noise present in OCT data is removed with a threshold.
- A Gaussian filter with $\sigma = 5$ is applied to create smooth contours and close small gaps in lumen boundary. Rays can miss a part of the lumen contour if it contains small gaps.

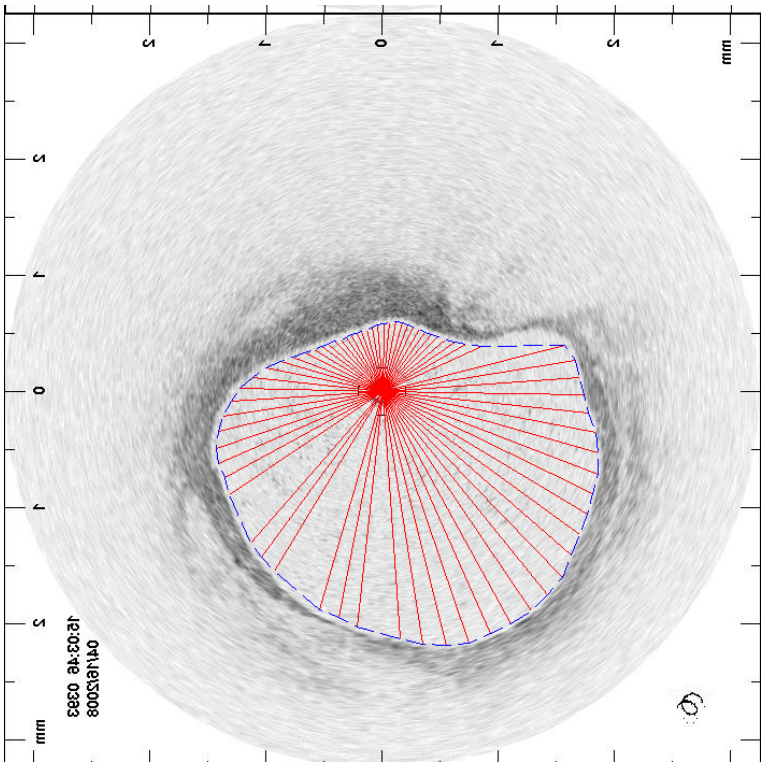

Figure 5.1: The angle between rays is 5 degrees, only rays are shown which successfully detected the lumen boundary.

5.2 Single Collision Ray

For every ray there exists at most one collision. All the collision points are connected to form the automatically detected contour. A collision is based on the following parameters:

- The lumen areas are usually brighter than the pixels within the lumen. A threshold for the image value is used.
- The image gradient is higher on edges than within areas. The image gradient magnitude is above a threshold.
- The Canny filter detects an edge.

For some OCT cross-sections this method works quite well (see fig. 5.1). However, the method is not robust against catheter artifacts around the center, noise present in OCT cross-sections, the guide wire and stents (see fig. 5.2).

5.3 Multiple Collisions Ray

To overcome the problems with the single collision rays the ray-casting is extended to multiple collisions per ray. This mostly solves the problem of catheter artifacts around the center, noise and the guide wire artifact.

At most one collision point has to be selected for every ray. Selecting the correct a collision point proved to be difficult for various cross-sections.

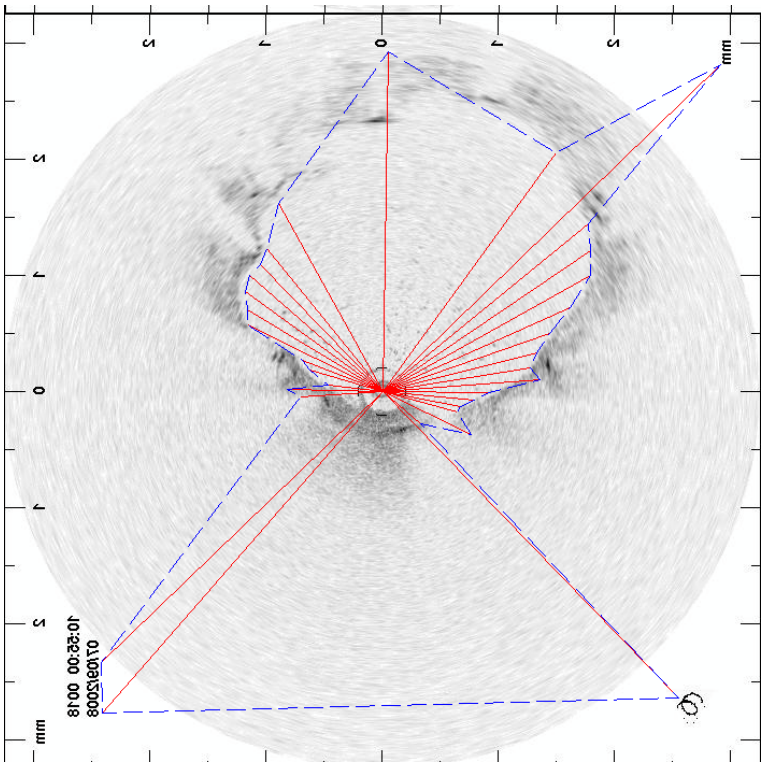

Figure 5.2: The angle between rays is 5 degrees, only rays are shown which successfully detected the lumen boundary. The contour detection is not robust and fails to correctly detect the lumen boundary.

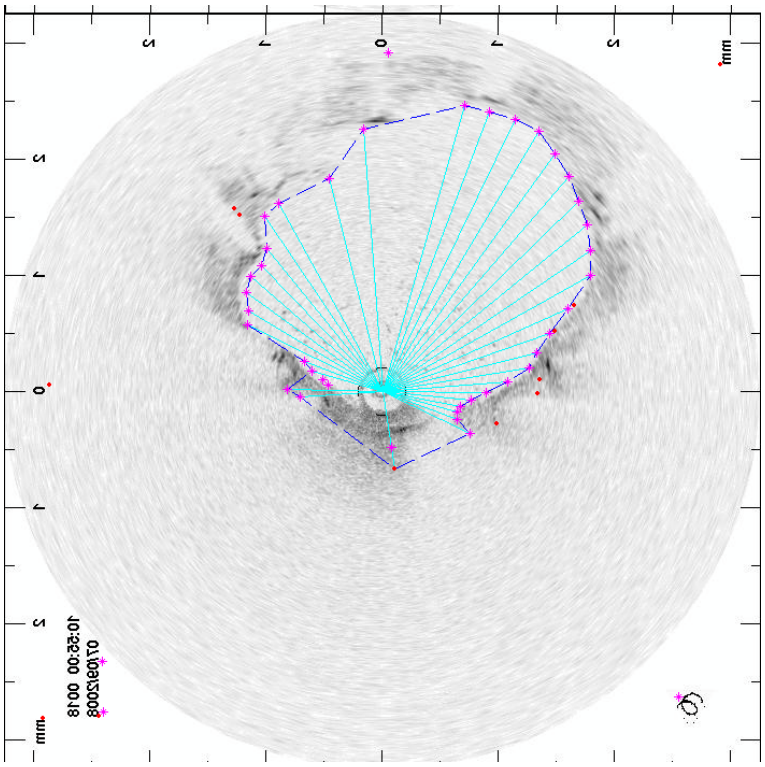

Figure 5.3: Multi ray-cast.

5.3.1 Choosing Collision Points Using Shortest Path

Our solution is to invert the polar coordinates and to find the shortest path through the inverted points. An added restriction, which is necessary to find a closed loop, is that the path has to go through all rays with collision points. Inverting the points before finding the shortest path has the effect of finding a path in the outer most points, this avoids selecting points detected from noise of catheter artifacts within the lumen area. The radial inversion can be mathematically described as follows:

$$\begin{aligned} p'_x &= L - \sqrt{p_x^2 + p_y^2}\cos(\arctan_2(p_y, p_x)) \\ p'_y &= L - \sqrt{p_x^2 + p_y^2}\sin(\arctan_2(p_y, p_x)) \end{aligned}$$

Where p'_x and p'_y are the x and y coordinates of the inverted point, L is a large number (larger than the distance between the center and the point farthest away from the center), p_x and p_y are the original points.

Although multiple collisions per ray improved the contour detection significantly (fig. 5.3). It still performs poorly on certain contours (fig. 5.4).

5.3.2 Skipping points

Not all rays with one or more collision points contain at least one point on the lumen boundary. Selecting any point on such rays will result in an incorrectly

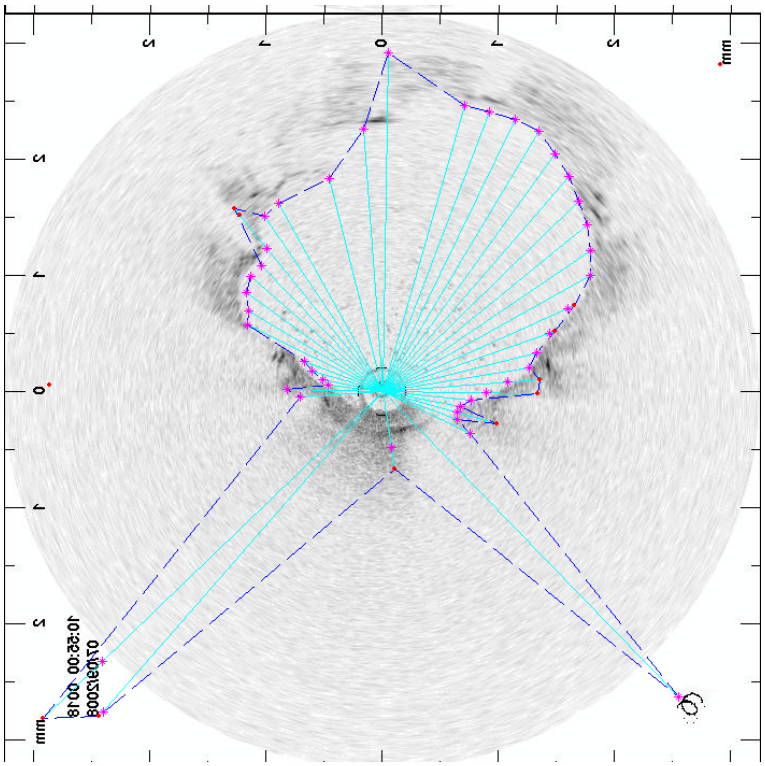

Figure 5.4: The points are radially inverted before

detected contour. An improvement can be made by skipping some collision points. Which points to skip is determined by the following heuristic:

$$r_{ij} = \alpha^{|j-i|} d_{ij} \tag{5.1}$$

where r_{ij} is a distance term heuristic, α is a constant (after trial and error we set this to 1.20), d_{ij} is the Euclidean distance between point i and point j. The term r_i is used to determine when points on the contour can be skipped (see fig. 5.4).

Example: the distance between the three consecutive points A, B and C are calculated where a, b and c are the indices of these points respectively and $[A + B]$ is the Euclidean distance between point A and Point B. Point B can lie far away from the lumen contour and from the points A and C. Point B is skipped on the contour if $[A + C] + r_{ac} < [A + B] + r_{ab}$ then point B is skipped otherwise it will be part of the contour. Where $\alpha^{|a-c|} = 1.20^{|1-3|} = 1.44$ and $\alpha^{|a-b|} = 1.20^{|1-2|} = 1.20$.

Although this heuristic improves the contour detection algorithm adjusting the it is error prone and often difficult to predict how any changes affect the resulting detected contour. Based on this we considered the ray-casting method to be unsuitable for accurate contour detection for OCT data.

5.4 Ray-casting discussion

The ray-casting technique worked well on some specific cross-sections but was difficult to improve across multiple cross-sections. The effect of tweaking specific parameters involved in improving the contour detection is often not obvious. The

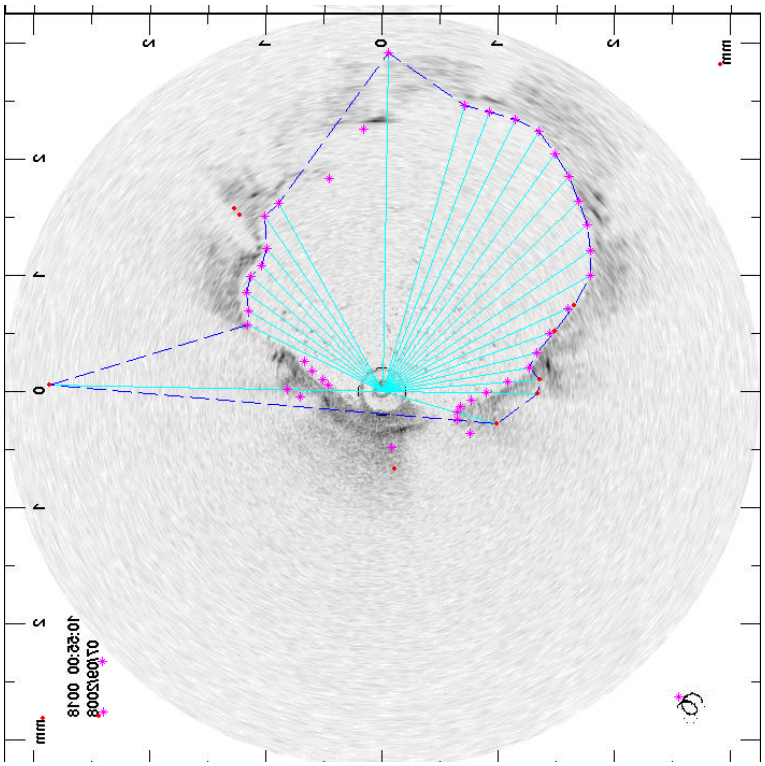

Figure 5.5: Skip heuristic used to improve the contour detection.

result of changing the parameters of the current contour detection algorithm is easier predict. The current contour detection algorithm includes or excludes edges instead of single contour points.

Using the center of the catheter guaranteed that all rays started from the inside of the lumen this property also proved to be useful for the suppression mask.

Chapter 6

Conclusion and Future Work

6.1 Conclusions

In this thesis, a viable automated lumen contour detection algorithm has been proposed and verified on 20 OCT data-sets. The contour detection can be used with our proposed gating algorithm to improve the accuracy for calculating the lumen volumes. As demonstrated in this thesis catheter movements caused by the cardiac cycle may affect the mean lumen area up to 15% with the fixed distance method. This can have a significant effect for studies that use a small number of data-sets. Our proposed gating algorithm may reduce this to less than 5%.

Second generation OCT called Optical Frequency Domain Imaging (OFDI) renders selection of end-diastolic cross-sections unusable. The catheter is quickly pulled back and the (near) end-diastolic cross-sections will lie far apart as a result. If it is possible to select end-diastolic cross-sections from such data-sets only very few cross-sections will be selected. However, the contour detection works correctly on these newer data-sets. However, OFDI is still a very new technique and not yet widely adopted, most data-sets are currently not generated using OFDI technology. OFDI may take over in the future, if this is the case then the gating algorithm will not be usable for newer OCT data-sets.

6.1.1 Limitations

For some cross-sections the lumen contour is incorrectly detected. However, these contours can be quickly located and fixed. Incorrectly detected contours are usually caused by branches in the coronary arteries. Correctly detecting the lumen area with a branch correctly is difficult, especially when the lumen boundary is closed. Sometimes contours are incorrectly detected when the catheter touches the vessel wall. The artifacts around the center of the catheter coincide with the vessel wall and can be mistakenly detected as part of the lumen contour.

Gating is used to improve the accuracy of calculating lumen volumes. Our gating algorithm has been verified on 12 data-sets out of 20 data-sets. Eight data-sets were discarded due to the absence of catheter movements that was apparent from the absence of saw-tooth shaped artifacts in the L-views. Plaque formation and calcification of the coronary arteries may lead to a reduced elasticity. As a result the lumen will not vary as much over the cardiac cycle this may contribute to less pronounced saw-tooth artifacts.

6.2 Future Work

Currently the data-sets have to be manually inspected before gating. If there are no clearly visible saw-tooth shaped artifacts in the L-views of an OCT data-set then the data-set is discarded as gating would most likely not provide a usable selection of cross-sections. Automatically discarding such data-sets could reduce the time required for calculating the lumen volume.

A golden standard does not exist for gating OCT data-sets (i.e. manually drawn lumen contours for automatic lumen contour detection). Instead a simulated pullback generating lumen contours could be used for verification of the gating method. The lumen volume would be known beforehand and can be compared to gated and non-gated methods. This simulation can also be used to compare different gating algorithms and to improve the current algorithm.

Bibliography

[1] G. J. Tearney, S. Waxman, M. Shishkov, B. J. Vakoc, M. J. Suter, M. I. Freilich, M. I. Freilich, W.-Y. Oh, L. A. Bartlett, M. Rosenberg, and B. E. Bouma, "Three-Dimensional Coronary Artery Microscopy by Intracoronary Optical Frequency Domain Imaging," *JACC Cardiovascular Imaging*, vol. 1, pp. 752–761, 2008.

[2] K. Sihan, C. Botha, F. Post, S. de Winter, E. Regar, R. Hamers, and N. Bruining, "A novel approach to quantitative analysis of intravascular optical coherence tomography imaging," pp. 1089–1092, 2008. http://www.cinc.org/Program/PC7-4.htm.

[3] K. Sihan, C. Botha, F. Post, S. de Winter, N. Gonzalo, E. Regar, P. J. Serruys, R. Hamers, and N. Bruining, "Fully automatic three-dimensional quantitative analysis of intracoronary optical coherence tomography." This paper is accepted but not published, 2009.

[4] T. H, S. P, C. TD, K. JD, V. DG, N. SE, and T. EM., "Influence of coronary pulsation on volumetric intravascular ultrasound measurements performed without ecg-gating. validation in vessel segments with minimal disease.," *International Journal of Cardiovasc Imaging*, vol. 19, pp. 51–57, 2003.

[5] K. Sihan, "A Survey of OCT Data Analysis," 2009.

[6] S. de Winter, "IntelliGate," Master's thesis, TU-Delft, 2003.

[7] R. Hamers, N. Bruining, M. Knook, M. Sabate, and J. Roelandt, "A novel approach to quantitative analysis of intravascular ultrasound images," in *Proceedings of Computers in Cardiology*, pp. 589–592, 2001.

Appendices

A Novel Approach to Quantitative Analysis of Intravascular Optical Coherence Tomography Imaging

K Sihan[1,2], C Botha[2], F Post[2], S de Winter[1],
E Regar[1], R Hamers[1], N Bruining[1]

[1]Erasmus MC, Rotterdam, The Netherlands
[2]TU-Delft, Delft, The Netherlands

Abstract

Quantitative analysis on intracoronary optical coherence tomography (OCT) image data (e.g. QOCT) is currently performed by a time-consuming manual contour tracing process in many individual OCT images acquired during a pullback procedure (frame-based method). In order to get a more efficient quantitative analysis process and to investigate the possibilities to use this contour information for development of an image-based retrospective OCT-gating method, as a first step a novel approach has been developed that exploits a full-automated contour tracing method for coronary lumens in OCT images without the need for intensive observer related actions.

This study presents this new method, which was tested on in-vivo acquired human coronary OCT image data of 10 randomly selected patients.

1. Introduction

The recent rapid developments in catheter based OCT technology have led to great enthusiasm towards applying this technique for the imaging of coronary artery disease and applying it to the evaluation of new therapeutic interventions. The major advantage of OCT over the current reference method for intracoronary imaging, intracoronary ultrasound (ICUS), is its exceptionally high image resolution, close to that of the golden standard of histopathology, i.e. lateral and axial resolutions of 15 and 25 µm respectively. In contrast, ICUS offers lateral and axial resolutions of 120 and 80 µm respectively [1]. To be able to select OCT for such evaluation purposes, quantitative analysis tools are imperative. The measurement accuracy of QOCT has been validated and showed a good correlation both with *ex-vivo* human coronary artery specimens as well as with *in-vivo* acquired OCT data [2]. The latter is far more tempting, since the imaging of the coronary vessel wall is impossible with OCT due to the presence of blood. The vessel must be occluded with a non-dilating balloon first and than flushed with saline, before OCT imaging becomes possible. Furthermore, induced motion artifacts caused by the cardiac cycle do not only cause in-plane artifacts (resulting in a sort of corkscrew appearance of the lumen contour) but also cause the saw-tooth shaped appearance of the coronary vessel wall. This limits the possibility of using reconstructed longitudinal views of the pullback OCT image dataset for contour detection, which would be much faster than analysis of each individual image [2]. Most acquired OCT image data sets contain multiple hundreds of frames. To analyze all frames is a time costly and tedious procedure currently taking up to multiple hours. Therefore many observers only analyze 1 frame per mm, randomly selected throughout the cardiac phase. This could result in a diminished accuracy for quantitative analysis.

To reduce the workload and to improve the accuracy by eliminating possible observer-related induced measurement inaccuracies, we investigated the possibility and feasibility of developing a fully automatic lumen contour detection approach. The newly developed method has been tested on *in-vivo* data of 10 patients with as reference method computer-assisted observer detected contours.

2. Methods

2.1. OCT imaging

We used OCT images acquired with a commercially available system (Lightlab Imaging, Westford, MA, USA). The light source was a 1310-nm broadband super luminescent diode with an output power in the range of 8.0 mW. The penetration depth in the tissue was approximately 1.5 mm. The imaging catheter (Imagewire™ Lightlab) had a maximum diameter of 0.019 inch and contained a single fiber optical core within a transluminent sheath. The wire was pulled back automatically at a speed of 1.0 mm/s while images were acquired at a rate of 15 frames/s. The acquired studies were saved in AVI format, and were then converted to DICOM by in-house developed dedicated software.

This article has been published as: Sihan, K.; Botha, C.; Post, F.; de Winter, S.; Regar, E.; Hamers, R. & Bruining, N. A Novel Approach to Quantitative Analysis of Intravascular Optical Coherence Tomography Imaging Proceedings of Computers in Cardiology, 2008, 1089-1092

Currently the OCT data still comes in different digital formats.

The developed fully automated OCT contour detection method contains the following steps:

2.2. Pre-processing

After importing the digitally stored OCT image data, a pre-processing filtering step is applied to every individual OCT image (Fig 1A). The primary goals of this step are to reduce speckle noise inherent in OCT data and to take care of gaps and shape irregularities in the blood-lumen interface. The preprocessing step consists of a combination of gaussian filtering and relative thresholds to remove speckle noise, morphological closing to remove gaps and contrast stretching to ensure that the image is properly normalized.

2.3. Edge detection

The basic algorithm used to detect all coronary vessel edges that can be found within a single OCT image, including the lumen edge (or boundary), is the Canny filter [3]. However, due to the rapid changes of the lumen morphology between sequential OCT images, a straightforward application of the Canny filter does not directly lead to the desired result. Furthermore, there is a large difference between the OCT datasets acquired from different individuals. To tackle these problems, the Canny filter is implemented iteratively using a binary search, until the desired percentage of image pixels are classified as edge pixels (Fig. 1). So the threshold of the Canny filter is increased or decreased depending on the amount of detected pixels.

2.3. Lumen edge selection

Not all edges detected by the Canny filter are on the lumen contour. Some edges are from noise caused by the catheter and some edges are from speckle noise. Even after the applied pre-processing some speckle noise will still be present in the images. Some parts of the contour may also not be visible or are not pronounced enough to produce an edge. In practice this is not such a problem judging by the fact that most contours are closed and clearly visible. The Canny filter also detects edges which do not belong on the lumen contour. These edges are removed using the dot product between the gradient orientation and the catheter center. So every pixel where this dot product is larger than a certain threshold is removed (fig. 1D). However, some erroneous edges are still present. The majority of these edges are short so a threshold by length is used to remove these edges. The subset of edges, which will be selected from the remaining edges, is the one providing with the highest quality score of all possible combinations. The quality parameter is determined by the area-, length- (relative to the area) and the gaps in the contour.

2.5. Post-processing

The pre-processing step sometimes pushes the edges detected with the Canny filter away from the lumen contour. In order to put the edges back on the lumen contour a post-processing step is applied. This step pushes contour points outwards based on the image gradient magnitude and a local search of 5 pixels. The contour is smoothed based on the radius length, weighting neighbour coordinates applying the gradient magnitude and the euclidean distance with a normal distribution.

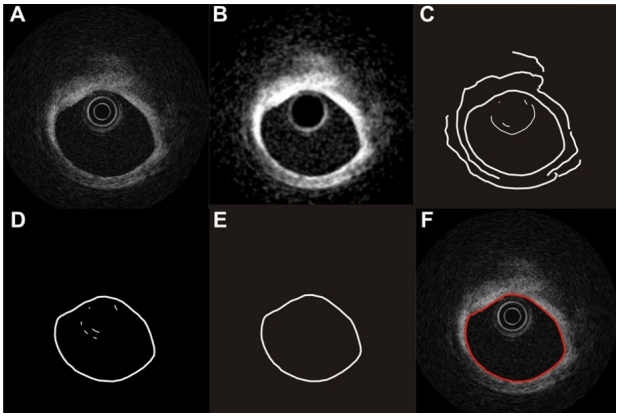

Figure 1. Panel A, shows an original OCT image. In panel B, the result of the pre-processing step can be appreciated and in panel C the edges diction results of the Canny filter. Panel D, shows the lumen contour edge selection and panel E the result after a threshold by edge length. Finally the lumen contour is presented in panel F.

3. Results

The new method was evaluated on 10 *in-vivo* acquired OCT pullback datasets of human coronary vessels. Every individual image was analyzed by a human observer using a computer-assisted software (Vessel analysis, CURAD BV, Wijk bij Duurstede, The Netherlands) and was used as reference method [2].

In these 10 datasets 1890 individual OCT images were available. The manual analysis required several hours and the automated method approximately 30-45 min (Fig. 2), resulting in a processing time of between 2-5 sec per

frame, depending on the image resolution. Of the 1890 automated detected lumen contours, 10 (0.5%) showed a large deviation as compared to the manual contours. The deviations were mostly caused by artifacts in the images, such as reflections of the outer sheath of the catheter. For possible necessary manual correction a graphical user interface is available.

The mean lumen areas of the 10 cases as measured by the human observer were 4.1±1.4 mm^2 and with the automated method 4.0±1.3 mm^2; p=0.09 (calculated by a student's t-test), respectively.

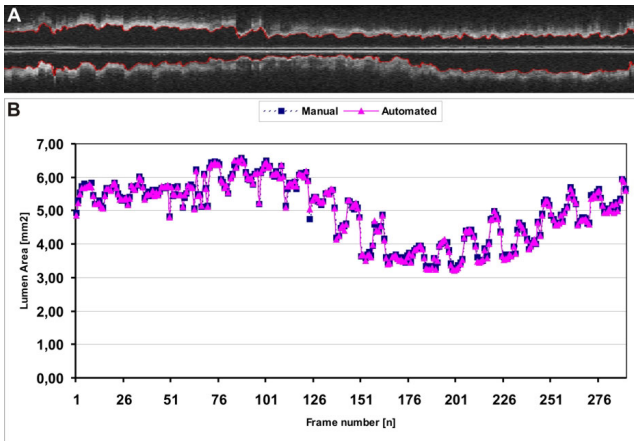

Figure 2. Panel A, shows a longitudinal reconstruction with the lumen contour presented on top of a total pullback procedure. Panel B shows the lumen area results of both methods.

Furthermore, linear regression analysis showed a good correlation between the methods (Fig. 3).

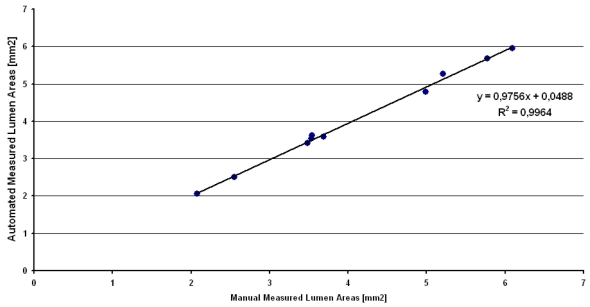

Figure 3. Linear regression analysis of the 10 cases.

Finally, also a Bland-Altman analysis showed good results without any outliers and with a mean relative difference between the methods of –1.14±1.87% (Fig. 4).

4. Discussion and conclusions

This study shows that the fully automated lumen contour detection of *in-vivo* human coronary OCT image data is feasible by showing similar results as a human observer without statistical significant differences.

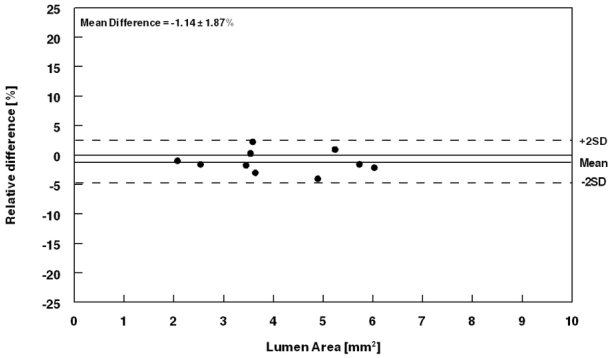

Figure 4. Bland-Altman analysis of the 10 cases.

However, there is a small tendency, resulting in a small systematic deviation, for the automated method to position the contour more at the inside of the lumen than on top of it, which seems to be the preference of the human observers. Since this is a systematic deviation, it plays no role in analysis of longitudinal studies and it was also not statistically significant.

To our knowledge this is the first fully automated OCT lumen contour detection method described. Although the number of cases used for this feasibility study is a bit on the low side, the results are promising. Although the fully automated method needs a check for deviated frames, the number of these false detected lumen contours is relatively very low (e.g. 0.5%). Furthermore, the applied quality score easily identifies those frames, so a complete visual check of all analyzed frames is not necessary.

The advantages of a fully automated contour detection method are the fast analysis time as compared to the manual method, although computer-assisted, and of course there are no inter- and intra-observer related possible deviations. Furthermore, the results of a fully automated lumen contour detection offer the possibility to use this for retrospective image-based OCT-gating. As can be appreciated in figures 2 and 5, the artifacts induced by the cardiac cycle cause a saw-tooth shaped appearance of the coronary vessel wall.

Since most cardiac imaging methods are gated it would be desirable to have also the possibility to gate OCT data since it improves not only the visual appearance (e.g. a smooth representation of the vessel wall providing a better matching with other imaging modalities as ICUS or multi-slice computed tomography (MSCT)) but also improves measurement accuracy [4]. Since OCT is becoming a popular choice for first-in-man trials for the evaluation of new therapeutic interventions,

accuracy is of utmost importance.

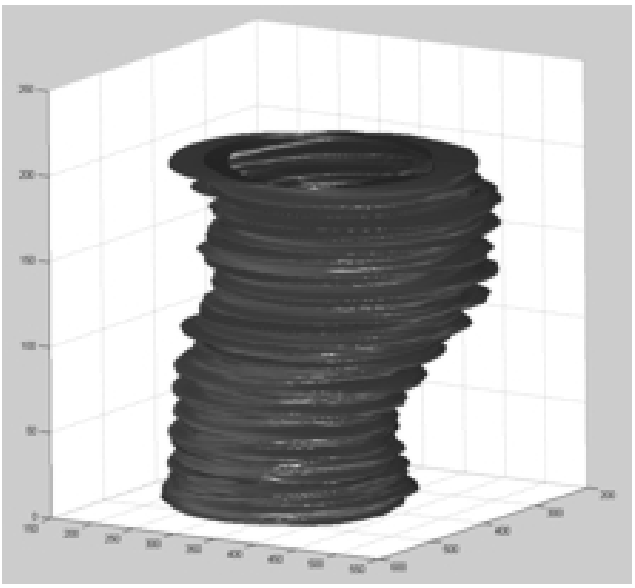

Figure 5. A 3D-plot of all full-automated detected lumen contours of 1 of the analyzed cases.

Previous studies have shown that OCT and QOCT are valuable additional imaging tools to the currently applied reference method for intravascular coronary imaging, ICUS. The advantages of OCT have been mentioned in the introduction. However, the current disadvantages are the necessary temporal closure of the vessel to be able to flush it with saline before the vessel wall can be imaged, and the low penetration depth limiting the visualization of the outer vessel borders in areas with severe amounts of plaque and finally cardiac motion induced artifacts. Retrospective image-based gating of which the current study was the first step could possibly solve the problem of motion artifacts [5].

For the first two problems, new systems are currently being developed and are in a research phase. They make use of the optical frequency domain imaging (OFDI) technique, allowing acquisition of images at the very high frame rate of approximately 125 frames/s. By pulling the catheter back at speeds of 15-25 mm/s at this high frame rate, the vessel does not need to be occluded anymore. However, these new advantages also bring new disadvantages. One of them is that in this way acquisition of images is performed during a few complete cardiac cycles bringing together images acquired at diastole and systole and everything in between. With the coronary lumen area changing on average 10% during the cardiac cycle this could lead to deviated results. This could limit the application of the OFDI technique in longitudinal atherosclerosis progression-regression trials. The current OCT technique combined with the possible application of gating could therefore provide a better platform when performing multi-modality imaging studies comparing the OCT image data against gated ICUS and gated MSCT data.

The present study shows that fully automated lumen contour detection in OCT images is feasible with a small number of frames showing easily correctible artifacts. The described method could be the first step towards a retrospective image-based OCT-gating method.

References

[1] Regar E, Schaar JA, Mont E, Virmani R, Serruys PW. Optical coherence tomography. *Cardiovascular radiation medicine.* Oct-Dec 2003;4(4):198-204.

[2] Tanimoto S, Rodriguez-Granillo G, Barlis P, de Winter S, Bruining N, Hamers R, Knappen M, Verheye S, Serruys PW, Regar E. A novel approach for quantitative analysis of intracoronary optical coherence tomography: high inter-observer agreement with computer-assisted contour detection. *Catheter Cardiovasc Interv.* Aug 1 2008;72(2):228-235.

[3] Canny J. A computational approach to edge detection. *IEEE transactions on pattern analysis and machine intelligence.* 1986;8:679-714.

[4] Bruining N, Tanimoto S, Otsuka M, Weustink A, Ligthart J, de Winter S, Van Mieghem CA, Nieman K, de Feijter PJ, van Domburg R, Serruys PW. Quantitative multi-modality imaging analysis of a bioabsorbable poly-l-lactic acid stent design in the acute phase: a comparison between 2- and 3D-QCA, QCU and QMSCT-CA. *Eurointervention.* 2008(August):285-291.

[5] De Winter SA, Hamers R, Degertekin M, Tanabe K, Lemos PA, Serruys PW, Roelandt JR, Bruining N. Retrospective image-based gating of intracoronary ultrasound images for improved quantitative analysis: The intelligate method. *Catheter Cardiovasc Interv.* Jan 2004;61(1):84-94.

Address for correspondence:

Nico Bruining
Erasmus MC/Room BA-571
Dr. Molewaterplein 40
3015 GD Rotterdam
The Netherlands
E-mail: n.bruining@erasmusmc.nl

Catheterization and Cardiovascular Interventions

e-mail print

SEARCH All Content Publication Titles Go

What is RSS?

Advanced Search
CrossRef / Google Search
Acronym Finder

Early View (Articles online in advance of print)

Published Online: 7 May 2009
Copyright © 2009 Wiley-Liss, Inc., A Wiley Company

Go to the homepage for this journal to access trials, sample copies, editorial and author information, news, and more.

Save Article to My Profile Download Citation

<Previous Article | Next Article >

Abstract | References | Full Text: HTML

View Full Width

Coronary Artery Disease

Fully automatic three-dimensional quantitative analysis of intracoronary optical coherence tomography†

Method and Validation

Kenji Sihan, BSc [1 2], Charl Botha, PhD [2], Frits Post, PhD [2], Sebastiaan de Winter, BSc [2], Nieves Gonzalo, MD [1], Evelyn Regar, MD, PhD [1], Patrick J.W.C. Serruys, MD, PhD [1], Ronald Hamers, PhD [1], Nico Bruining, PhD [1 *]

[1]Thoraxcenter, Delft, The Netherlands

[2]Department of Cardiology, Erasmus MC, Rotterdam, The Netherlands and TU-Delft, Delft, The Netherlands

email: Nico Bruining (n.Bruining@erasmusmc.nl)

[*]Correspondence to Nico Bruining, Erasmus MC, P.O. Box 1738, 3000 DR Rotterdam, The Netherlands

† Conflict of interest: Dr. Hamers is an employee of CURAD BV, Wijk Bij Duurstede, The Netherlands.

KEYWORDS

angiography • coronary • diagnostic cardiac catheterization • quantitative vascular angiography

ABSTRACT

Objectives and background: Quantitative analysis of intracoronary optical coherence tomography (OCT) image data (QOCT) is currently performed by a time-consuming manual contour tracing process in individual OCT images acquired during a pullback procedure (frame-based method). To get an efficient quantitative analysis process, we developed a fully automatic three-dimensional (3D) lumen contour detection method and evaluated the results against those derived by expert human observers. Methods: The method was developed using Matlab (The Mathworks, Natick, MA). It incorporates a graphical user interface for contour display and, in the selected cases where this might be necessary, editing. OCT image data of 20 randomly selected patients, acquired with a commercially available system (Lightlab imaging, Westford, MA), were pulled from our OCT database for validation. Results: A total of 4,137 OCT images were analyzed. There was no statistically significant difference in mean lumen areas between the two methods (5.03 ± 2.16 vs. 5.02 ± 2.21 mm^2; $P = 0.6$, human vs. automated). Regression analysis showed a good correlation with an r value of 0.99. The method requires an average 2-5 sec calculation time per OCT image. In 3% of the detected contours an observer correction was necessary. Conclusion: Fully automatic lumen contour detection in OCT images is feasible with only a select few contours showing an artifact (3%) that can be easily corrected. This QOCT method may be a valuable tool for future coronary imaging studies incorporating OCT. © 2009 Wiley-Liss, Inc.

Received: 25 March 2009; Accepted: 23 April 2009

DIGITAL OBJECT IDENTIFIER (DOI)

10.1002/ccd.22125 About DOI

ARTICLE TEXT

INTRODUCTION

Optical coherence tomography (OCT) has been rapidly accepted as an additional invasive coronary imaging tool [[1]]. It allows highly

This article has been accepted as: Sihan, K.; Botha, C.; Post, F.; de Winter, S.; Gonzalo, N.; J.W.C. Serruys P.; Regar, E.; Hamers, R. and Bruining, N. Fully automatic three-dimensional quantitative analysis of intracoronary optical coherence tomography, Catheterization and Cardiovascular Interventions.

detailed imaging of the coronary lumen and vessel wall morphology at resolutions of 10 times higher than what current intracoronary ultrasound (ICUS) can offer. The details shown within OCT images are close to histopathology, allowing accurate evaluation of by example apposition of stent struts and--in longitudinal studies--tissue-coverage of drug-eluting stents (DES) [[2]]. This advantage has resulted in an increasing use of OCT in studies evaluating new therapeutic treatments, in addition to ICUS, the current de facto reference method for intravascular imaging [[3][4]].

To apply an imaging method in studies, accurate quantitative analysis tools are required, as has been proven by quantitative angiography (QCA) [[5]] and quantitative ICUS (QCU) [[6][7]]. Recently, results of computer-assisted quantitative OCT (QOCT) have been reported showing good results for coronary lumen measurements [[8]]. However, because an OCT examination contains hundreds of individual images, such analysis can, despite the use of computer-assisted tools, be a tedious and time-consuming process [[8]]. However, because the lumen-intima interface is so clearly visualized in OCT, far better than in ICUS, a fully automatic lumen contour detection approach could be feasible.

This article reports on a novel in-house developed fully automatic three-dimensional (3D) OCT lumen contour detection approach and its validation using expert human observer computer-assisted analysis as a reference.

MATERIALS AND METHODS

OCT Imaging System

OCT imaging was performed with a commercially available system (Lightlab imaging, Westford, MA). This system uses a 1,310-nm broadband light-source generated by a super luminescent diode with an output power in the range of 8.0 mW. The average tissue penetration depth is approximately 1.5 mm with an axial and lateral resolution of 15 and 25 μm, respectively. The imaging probe has the size of a guide-wire with a maximum outer diameter of 0.019 inch (Imagewire^{TM}, LightLab Imaging). The wire contains a single-mode fiber optic core within a translucent sheath. The imaging-wire is connected to an imaging console, similar as ICUS, which performs the real-time image data processing, visualization, and image storage. Systematic imaging of a coronary segment is also analogue to ICUS by an automatic continuous speed pullback (between 1 and 3 mm/sec) of the imaging wire [[6]]. OCT images are generated at a rate of 10-20/sec (cf. ICUS 30 frames/sec). The accuracy of OCT for dimensional measurements--determined using a phantom--has been recently reported to be excellent (mean difference in measured length of -0.03 mm with 0.02 mm precision) [[8]].

Patients and OCT Image Acquisition

For validation of the automated method, we made a random selection of 20 OCT cases from our database of patients participating in different studies. In all cases a standard femoral approach with 7F guiding catheters was used. Before imaging, all patients received weight-adjusted heparin intravenously to maintain an activated clotting time of >300 sec as well as intravenous analgesics. To be able to see the coronary vessel wall, the coronary artery must be cleared of blood by replacing it with lactated Ringer's solution. This procedure is performed by occlusion of the artery with a dedicated occlusion catheter (Helios, Goodman, Japan) including a short balloon (6.0 mm length) that can be inflated by a low pressure (0.3 atm). The Ringer's is infused distally from the balloon at a rate of 0.5 ml/sec at a temperature of 37°C). Sufficient occlusion of the coronary is checked by contrast injection via the guiding catheter and the balloon pressure is increased (at 0.5 atm increments) when necessary. The images were digitally stored in the AVI file format on DVD's and were translated later into the DICOM medical imaging standard by in-house developed software.

Automated Quantitative OCT Method

The automated OCT lumen contour detection method was developed in the Matlab environment (The Mathworks, Natick, MA). The method has five stages:

Preprocessing

Each individual OCT frame is preprocessed to remove speckle noise and gaps and to adapt the contrast for proper image normalization. Prepocessing consists of the application of a Gaussian filter and using different relative thresholds (Fig. 1B). The relative thresholds are applied on the pixel values to remove extreme values and to improve image normalization.

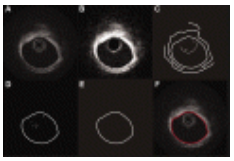

Figure 1. This figure shows the results of the different processing steps. (A) An original OCT image is presented. (B) The image after the application of a Gaussian filter. (C) The detected edges as a result of the iteratively applied Canny filter. (D) The remaining edges after application of the angle constraint. Short edges are removed after application of a length threshold (E). The postprocessed and smoothed final contour is presented in (F). [Color figure can be viewed in the online issue, which is available at www.interscience.wiley.com.]
[Normal View 30K | Magnified View 110K]

Edge detection

A Canny [[9]] filter is applied to detect edges in the OCT image. The final lumen contour is the result of appropriately selected edges, which are positioned on the lumen-intima border only. Straightforward application of the standard Canny filter to the OCT images leads to many false and/or missed contours. Therefore, we iteratively apply the Canny filter to match the constraints necessary for OCT images (percentage of image pixels classified as true edges). This percentage is based on a test-set where it is set in such a way that the lumen contour is detected while detecting as little noise as possible. Within this procedure, the threshold of the Canny filter is optimized using a binary search algorithm.

Lumen edge selection

The result of the Canny edge detection stage includes some edges that do not belong to the lumen-intima interface, for example radially behind bright areas (Fig. 1C). These false edges are mostly due to noise caused by the catheter and by speckle noise which was not be removed by the preprocessing step without significantly impairing image details. The majority of these false edges are identified by two constraints:

1. The angle between the gradient orthogonal to the line segment and the line connecting it to the catheter center should be smaller than a certain threshold.
2. The length of the edge should be longer than a certain threshold (Fig. 1).

Lumen edge linking

The final lumen contour is the optimal combination of the resulting true edges. This is performed using a quality score determined by the resultant lumen area, length (relative to the area), and gaps in the contour (relative to the length). For all possible combinations of edge selections, the quality score is calculated and the combination with the highest score results in the final lumen contour.

Postprocessing

Postprocessing is applied to overcome possible errors introduced by the pre-processing and those inherent to the nature of OCT imaging itself (such as large side-branches, gaps caused by guide-wire artifacts, etc.). The postprocessing is divided into several subprocesses:

Contour correction and smoothing

The iterative application of the Canny filter does not select the edges with local maximum gradient. In a postprocessing step, the maximum gradient search is automatically performed within a 5 pixel radius from the initially found contour. Subsequently, the contour is smoothed, weighing neighbor coordinates with the gradient magnitude in a normal distribution.

Side-branch gaps and out-of-range borders

The resulting luminal contours may still have gaps, which are mostly caused by side-branches and/or guide-wire artifacts. Furthermore, often in OCT images the lumen border is out of range, in large vessels, or is not pronounced enough to produce an edge (Fig. 2). To close these gaps and omissions, a mathematical circular correction model is applied (Fig. 2).

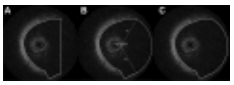

Figure 2. To close the remaining gaps, the straight line at the right-hand side (A), a circular arc interpolation is performed automatically using the center of gravity of the contour as the center of the circle (B). For the radius, linear interpolation is used from r1 to r2. The repaired contour is presented in (C).
[Normal View 35K | Magnified View 148K]

Replacement of falsely detected contours (3D analysis)

In the case of large side-branches, heavy noise or large parts of missing visible lumen data within the OCT images (Fig. 3), it is still possible that the automated contour detection does not result in the desired contour. For each consecutive image, the enclosed area of the lumen contour is calculated. Frames showing a relatively large deviation in areas compared to their neighbors are labeled as incorrect. A search and substitute algorithm replaces these contours by the closest available correct contour in the longitudinal direction.

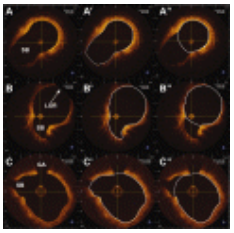

Figure 3. This figure presents a few different lumen morphologies which are difficult to detect correctly fully-automated. (A) A large side-branch can be appreciated (indicated by SB). (A') The detected automated contour, which has been corrected by the human observer (A″). (B) In addition to a side-branch also a case were part of the lumen is out of range for the OCT catheter. The automated contour detection applied the automated circular correction (B') and the human observer corrected for the large side-branch artifact (B″). Finally, in (C) a guide-wire artifact is presented (C, GA). This relatively small gap is automatically repaired by the correction algorithms (C'). Again, also in this example the observer corrected for the large side-branch (C″). [Color figure can be viewed in the online issue, which is available at www.interscience.wiley.com.]
[Normal View 71K | Magnified View 311K]

Final approval and correction

It is very difficult, or even impossible, to develop a 100% accurate fully automatic detection method in medical image processing. The large differences found in coronary morphology will always result in unexpected images that could not have been foreseen during development. Therefore, the results must be validated by an expert. To facilitate this, a user interface was developed, similar to that used for QCU [[10]].

Validation

For validation of the automated method, the quantitative results were compared against those derived by application of a computer-assisted lumen detection method (CURAD vessel analysis, CURAD BV, Wijk bij Duurstede, The Netherlands) [[8]]. The expert (N.G.) was blinded for the automated results.

Statistical Analysis

Quantitative data are presented as mean ± standard deviation (SD). Comparison between the methods was performed by the two-tailed paired Student's *t*-test. A *P* value < 0.05 was considered statistically significant. In addition, regression analysis and the method as proposed by Bland and Altman [[11]] was performed.

RESULTS

In the 20 OCT cases a total of 4,167 frames were analyzed (208 ± 92 frames on average per patient). In each case, the OCT images were analyzed consecutively, without intervals (Fig. 4). Although the human analysis time was not measured, it is well known that this is usually a lengthy process. The automated method required on average approximately 2-5 sec of calculation time per frame. In 125 OCT frames (3%), the automatic results had to be corrected.

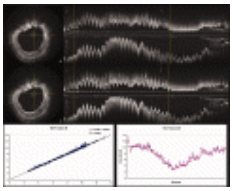

Figure 4. A typical analysis example is presented. In (A) an individual cross-sectional image is shown and in (A') the longitudinal reconstruction of the pullback examination. In (B and B'), the same images are presented with the automated contour detected result superimposed. It can be appreciated that the cross-sectional OCT images present a lot of details of the lumen-intima morphology. (C) The regression analyses of the area measurements of all frames with the manual results on the *x*-axis and the automated results on the *y*-axis. Finally in (D), all the area measurements are presented of both methods. [Color figure can be viewed in the online issue, which is available at www.interscience.wiley.com.]
[Normal View 82K | Magnified View 351K]

The computer-assisted manual analysis showed a mean lumen area of 5.0 ± 2.2 mm^2 versus 5.1 ± 2.2 mm^2 for the fully automatic method, with no statistical significant difference (*P* = 0.26). The relative difference was 0.4% ± 1.8%. Regression analysis yielded *r* = 0.999 (Fig. 5).

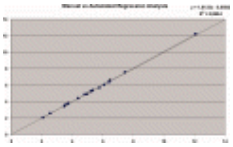

Figure 5. The linear regression analysis for the 20 OCT cases analysed computer-assisted (e.g., manual) versus fully automatic. [Color figure can be viewed in the online issue, which is available at www.interscience.wiley.com.]
[Normal View 21K | Magnified View 65K]

Bland and Altman analysis revealed a single outlier (Fig. 6). All other cases were within an interval of ±2%. Inspection of the outlier showed a deviated contour detection by the expert observer, which resulted in a relative difference of 6%. If this outlier is disregarded, the results are 5.1 ± 2.2 mm^2 (expert) versus 5.1 ± 2.2 mm^2 (automated), *P* = 0.52; relative difference 0.02% ± 1.1%.

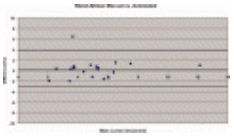

Figure 6. The relative differences according to the method as proposed by Bland and Altman [[11]]. [Color figure can be viewed in the online issue, which is available at www.interscience.wiley.com.]
[Normal View 23K | Magnified View 72K]

DISCUSSION

This study shows that fully automatic 3D lumen contour detection for quantitative OCT analysis is feasible. The quantitative results are similar to those derived manually by an expert.

To evaluate new interventional therapies, quantitative imaging tools are mandatory, such as QCA [[5]] and QCU [[6][10]]. Although a computer-assisted method for QOCT has been presented showing excellent results [[8]], the advantages of fully automatic contour detection are obvious. It does not consume the valuable time of an expert neither does it suffer from possible interobserver- and intraobserver-related deviations. Furthermore, as the outlier case in this report shows, contours which are not precisely positioned on the lumen border can result in a relatively large deviation (in this case 6%). The human expert will most likely be more motivated to analyze all images in a pullback (and not a limited subset of images selected at by example 1 mm intervals, e.g. every 15th frame) if the majority of the contours are already correctly detected and the human effort required is purely for inspection and a limited number of corrections (Fig. 3).

OCT is a relatively new coronary imaging technique, but it has gained considerable enthusiasm in a very short period. It can reveal much more information of the region around the lumen border than is achievable with the current available ICUS technology. However, on the down-side, the penetration depth into the coronary vessel wall and present plaques is still limited (1-2 mm). Therefore, at this moment an automated outer vessel contour detector cannot be developed. Furthermore, because OCT cannot be used to perform coronary plaque measurements, the advantages and disadvantages of OCT in several different clinical scenarios have been described recently [[8]].

At present, several different commercial OCT systems are available. For this study the system of Lightlab was used [[12][13]]. This system has an integrated quantitative analysis tool that is limited to single frames. Furthermore, to our knowledge the method has not been published. This single frame approach requires a time consuming and operator dependent manual frame selection at 1 mm intervals. It has been reported that depending on the length of the analyzed region it can take up 2-4 hr to complete an analysis [[8]].

Independent third party quantitative software tools are, to our knowledge, not yet reported, except for one study presented by Tanimoto et al. [[8]]. In this article, a computer-assisted dedicated OCT analysis tool was reported, showing good inter and intraobserver quantitative results (1.57% ± 0.05% for lumen areas). However, only well-visualized OCT images were included. Images suffering from motion-induced artifacts, dissections, and side-branches--hampering analysis--were excluded (9%). In this study, all available imaging data (real world data) was analyzed and no exclusions were made. To our knowledge, to date, no other reports have been published concerning fully automatic QOCT methods.

Limitations

Unfortunately, because of the nature of OCT, the penetration depth is currently to low to be able to visualize the coronary vessel wall in diseased segments and therefore only the coronary lumen could be quantified in this study. Developments of newer OCT methods, such as OFDI, and application of other light sources, could possibly enhance the penetration depth making it hopefully possible to visualize advanced coronary plaques in the near future.

The number of cases included in this study is limited, a larger number of cases must reveal if the excellent score of fully automatic detection in 97% of the images can be maintained for larger populations. However, we evaluated almost 4,200 individual OCT images of very different lumen morphology, because of the high spatial resolution.

Future Developments

This full-automated approach to quantify the coronary lumen by OCT is the first step towards further developments of highly anticipated additional quantification tools. On the requirements list are currently: detection of stent struts, protrusion of plaque contents through stent struts, in-stent thrombi, fibrous caps (detection and thickness measurements), and plaque composition. If these requirements could be detected automatically remains topic for further research and developments. However, measurements of in-stent intima hyperplasia, lumen-eccentricity and -remodeling (if base-line and follow-up OCT measurements are available) are already possible using the automated approach (for lumen) in combination by computer-assisted tools (for stent contouring) [[8]].

The described method has been developed in a generic mathematical research environment on a normal desktop personal computer running Microsoft Windows. The processing time of 2-5 sec could most likely be reduced in the near future if the software were to be ported to a dedicated QOCT environment.

Many of the OCT images suffer from motion artifacts, which are caused by the low temporal resolution of current OCT systems as compared to the relatively rapid motion of the heart. The heart motion also causes the saw-tooth shaped appearance of the coronary vessel wall in the longitudinal reconstructions (Fig. 4). These motion-related artifacts could probably be overcome by the application of optical frequency domain imaging (OFDI) to coronary vessel imaging. However, these systems are still in the research phase and not commercially available yet.

CONCLUSION



This study shows that fully automatic lumen contour detection in OCT images is feasible with only a few contours showing an artifact (3%) that can be easily corrected. This QOCT method may be a valuable tool for future coronary imaging studies incorporating OCT.

REFERENCES



1 Regar E, Schaar JA, Mont E, Virmani R, Serruys PW. Optical coherence tomography. *Cardiovasc Radiat Med* 2003; **4**: 198-204. Links

2 Prati F, Zimarino M, Stabile E, Pizzicannella G, Fouad T, Rabozzi R, Filippini A, Pizzicannella J, Cera M, De Caterina R. Does optical coherence tomography identify arterial healing after stenting? An in vivo comparison with histology, in a rabbit carotid model. *Heart* 2008; **94**: 217-221. Links

3 Guagliumi G, Sirbu V. Optical coherence tomography: High resolution intravascular imaging to evaluate vascular healing after coronary stenting. *Catheter Cardiovasc Interv* 2008; **72**: 237-247. Links

4 Ormiston JA, Serruys PW, Regar E, Dudek D, Thuesen L, Webster MW, Onuma Y, Garcia-Garcia HM, McGreevy R, Veldhof S. A bioabsorbable everolimus-eluting coronary stent system for patients with single de-novo coronary artery lesions (ABSORB): A prospective open-label trial. *Lancet* 2008; **371**: 899-907. Links

5 Haase J, Escaned J, van Swijndregt EM, Ozaki Y, Gronenschild E, Slager CJ, Serruys PW. Experimental validation of geometric and densitometric coronary measurements on the new generation Cardiovascular Angiography Analysis System (CAAS II). *Cathet Cardiovasc Diagn* 1993; **30**: 104-114. Links

6 Mintz GS, Nissen SE, Anderson WD, Bailey SR, Erbel R, et al. American College of Cardiology Clinical Expert Consensus Document on Standards for Acquisition, Measurement and Reporting of Intravascular Ultrasound Studies (IVUS). A report of the American College of Cardiology Task Force on Clinical Expert Consensus Documents. *J Am Coll Cardiol* 2001; **37**: 1478-1492. Links

7 von Birgelen C, Mintz GS, Nicosia A, Foley DP, van der Giessen WJ, Bruining N, Airiian SG, Roelandt JRTC, de Feyter PJ, Serruys PW. Electrocardiogram-gated intravascular ultrasound image acquisition after coronary stent deployment facilitates on-line three-dimensional reconstruction and automated lumen quantification. *J Am Coll Cardiol* 1997; **30**: 436-443. Links

8 Tanimoto S, Rodriguez-Granillo G, Barlis P, de Winter S, Bruining N, Hamers R, Knappen M, Verheye S, Serruys PW, Regar E. A novel approach for quantitative analysis of intracoronary optical coherence tomography: High inter-observer agreement with computer-assisted contour detection. *Catheter Cardiovasc Interv* 2008; **72**: 228-235. Links

9 Canny J. A computational approach to edge detection. *IEEE Trans Pattern Anal Mach Intel* 1986; **8**: 679-714. Links

10 Hamers R, Bruining N, Knook M, Sabate M, Roelandt JRTC. A novel approach to quantitative analysis of intravascular ultrasound images. *Comput Cardiol* 2001: 589-592. Links

11 Bland JM, Altman DG. Statistical methods for assessing agreement between two methods of clinical measurement. *Lancet* 1986; **1**: 307-310. Links

12 Matsumoto D, Shite J, Shinke T, Otake H, Tanino Y, Ogasawara D, Sawada T, Paredes OL, Hirata K, Yokoyama M. Neointimal coverage of sirolimus-eluting stents at 6-month follow-up: Evaluated by optical coherence tomography. *Eur Heart J* 2007; **28**: 961-967. Links

13 Takano M, Inami S, Jang IK, Yamamoto M, Murakami D, Seimiya K, Ohba T, Mizuno K. Evaluation by optical coherence tomography of neointimal coverage of sirolimus-eluting stent three months after implantation. *Am J Cardiol* 2007; **99**: 1033-1038. Links